Additional Amphivasal Bundles in Pedicel Pith Exacerbate Central Fruit Dominance and Induce Self-Thinning of Lateral Fruitlets in Apple[1][C][W]

Jean-Marc Celton*, Emmanuelle Dheilly, Marie-Charlotte Guillou, Fabienne Simonneau, Marjorie Juchaux, Evelyne Costes, François Laurens, and Jean-Pierre Renou

Institut National de la Recherche Agronomique, Unité Mixte de Recherche 1345 Institut de Recherche en Horticulture et Semences, 49071 Beaucouzé, France (J.-M.C., E.D., M.-C.G., F.S., M.J., F.L., J.-P.R.); AgroCampus-Ouest, Unité Mixte de Recherche 1345 Institut de Recherche en Horticulture et Semences, 49045 Angers, France (J.-P.R.); Université d'Angers, Unité Mixte de Recherche 1345 Institut de Recherche en Horticulture et Semences, Structure Fédérative de Recherche 4207 Qualité et Santé du Végétal, 49045 Angers, France (J.-P.R.); and Institut National de la Recherche Agronomique, Unité Mixte de Recherche 1334, Amélioration Génétique et Adaptation des Plantes Méditerranéennes et Tropicales Centre International de Recherche Agronomique pour le Développement-Institut National de la Recherche Agronomique-Montpellier SupAgro, TA A 96/03, 34398 Montpellier cedex 5, France (E.C.)

Apple (*Malus* × *domestica*) trees naturally produce an excess of fruitlets that negatively affect the commercial value of fruits brought to maturity and impact their capacity to develop flower buds the following season. Therefore, chemical thinning has become an important cultural practice, allowing the selective removal of unwanted fruitlets. As the public pressure to limit the use of chemical agents increases, the control of thinning becomes a major issue. Here, we characterized the self-thinning capacity of an apple hybrid genotype from the tree scale to the molecular level. Additional amphivasal vascular bundles were identified in the pith of pedicels supporting the fruitlets with the lowest abscission potential (central fruitlet), indicating that these bundles might have a role in the acquisition of dominance over lateral fruitlets. Sugar content analysis revealed that central fruitlets were better supplied in sorbitol than lateral fruitlets. Transcriptomic profiles allowed us to identify genes potentially involved in the overproduction of vascular tissues in central pedicels. In addition, histological and transcriptomic data permitted a detailed characterization of abscission zone development and the identification of key genes involved in this process. Our data confirm the major role of ethylene, auxin, and cell wall-remodeling enzymes in abscission zone formation. The shedding process in this hybrid appears to be triggered by a naturally exacerbated dominance of central fruitlets over lateral ones, brought about by an increased supply of sugars, possibly through additional amphivasal vascular bundles. The characterization of this genotype opens new perspectives for the selection of elite apple cultivars.

Abscission is a dynamic process in plants that consists of the detachment of organs such as leaves, flowers, and fruits by the separation of cells in anatomically distinct regions called abscission zones (AZs). The current model of abscission defines four major stages: (1) differentiation of the AZ at the future site of detachment; (2) acquisition of competence to react to abscission signals; (3) activation of the abscission process within the AZ; and (4) differentiation of a protective layer on the surface of the separation layer at the plant's side (Patterson, 2001). Various studies have shown that to induce the abscission process, AZs are rendered more sensitive to ethylene because of a decreased production of auxin by the subtending organ and subsequent translocation down the petiole (Taylor and Whitelaw, 2001; Meir et al., 2010; Zhu et al., 2011). The phytohormone ethylene is thought to stimulate cells to produce enzymes that degrade the middle lamella between cells in the AZ (Mao et al., 2000). Several species, particularly fruit trees, set excess flowers that produce a surplus of fruits that the plant is not always able to support to maturity. To reduce fruit load, fruit trees, and particularly apple (*Malus* × *domestica*) trees, have developed a mechanism whereby they shed part of their fruit load to guarantee the completion of the fruit ontogenetic program (Dal Cin et al., 2009). This process, called physiological drop, occurs during the early phases of fruit development, with kinetics that may change according to the species, the physiological state of the plant, and various environmental

[1] This work was supported by the Région Pays de la Loire, the Angers agglomeration, and the Institut National de la Recherche Agronomique.

* Address correspondence to jean-marc.celton@angers.inra.fr.

The author responsible for distribution of materials integral to the findings presented in this article in accordance with the policy described in the Instructions for Authors (www.plantphysiol.org) is: Jean-Marc Celton (jean-marc.celton@angers.inra.fr).

[C] Some figures in this article are displayed in color online but in black and white in the print edition.

[W] The online version of this article contains Web-only data.

www.plantphysiol.org/cgi/doi/10.1104/pp.114.236117

factors (Bonghi et al., 2000). In young developing fruits, the abscission is mainly due to a correlative dominance effect that describes the mutual interactions between individual organs (adjacent fruits or nearby shoots) and their dependency on one another (Bangerth, 2000).

Apple trees have the characteristic to develop flowers and fruits organized in clusters called corymbs. Corymbs are usually composed of four to six fruits attached to a floral growth unit (the bourse, a short shoot that forms the basis from which all flowers/fruits of a corymb develop) via pedicels. These corymbs are interesting models in which to study physiological drop, since they display a gradient of correlative dominance in relation with the position of the fruit in the cluster. In this model, the central fruitlet (the central position and most distal from the corymb base) exerts a dominance over the laterals, which can be classified by their relative position and size as big lateral fruitlet (L3, the lateral fruit closest to the central fruit), itself dominant over the medium (L2) and small lateral fruitlets (L1, the lateral fruit closest to the corymb base; Botton et al., 2011). Horticulturists can exacerbate this dominance (1) by treatment with chemicals that induce fruit drop or (2) by means of shading (Greene et al., 1992; Bangerth, 2000). This practice, called fruit thinning, is widely adopted by fruit growers to reduce the number of fruits on the tree, and chemical thinning has become a common practice in orchard management in order to meet consumers' criteria of fruit size and quality and to reduce the biennial bearing behavior. Benzyladenine and metamitron are widely used chemical thinners that exert their action by stimulating shoot growth, which in turn increases fruit drop by exacerbating competition between shoots and corymbs, between the different corymbs, and, more importantly, between fruits of the same corymb (Bangerth, 2000; Bubán, 2000). However the effect of chemical thinners largely depends on cultivar and environmental conditions and may present a threat to the environment, stimulating the demand for alternative strategies such as the selection of new cultivars with self-thinning properties.

In apple, the natural physiological drop starts 2 to 3 weeks after petal fall and culminates a few weeks later with an increased activity of cell wall-degrading enzymes occurring in preformed cell layers forming the AZ (Gonzáles-Carranza et al., 2002). The physiological drop has to be distinguished from the senescence-driven abscission of ripe fruits (Bangerth, 2000). In Arabidopsis (*Arabidopsis thaliana*) and tomato (*Solanum lycopersicum*), the activities of cell wall-degrading enzymes have been shown to increase dramatically with the onset of abscission, including cellulase, polygalacturonase, expansin, and xyloglucan endohydrolase endotransglycosylase (Lashbrook et al., 1994; Kalaitzis et al., 1997; Agustí et al., 2008, 2009; Cai and Lashbrook, 2008; Roberts and González-Carranza, 2009).

The selective drop of fruitlets can be interpreted as a developmental arrest that the plant exerts on particular young fruits during early phases of development (Bangerth, 2000). Hence, in response to nutritional shortage, fruitlets representing the weaker sinks are induced to abscise. Tests on various apple cultivars showed that fruitlet abscission occurred if the growth rates were not maintained above 60% of the rate of the fastest growing fruitlet in a population (Lakso et al., 2001).

Results from recent studies based upon transcriptomic and metabolomic data have permitted the development of a model that links abscission induction and the nutritional stress occurring within the tree (Botton et al., 2011; Eccher et al., 2013). In this model, the fruitlet cortex perceives the altered physiological conditions, and the molecular mechanisms linking sugar starvation to hormonal signaling are activated. As a consequence, abscisic acid and ethylene signaling pathways are strongly up-regulated concurrently with a down-regulation of GA signaling in the fruitlet induced to abscise.

From this model, we can assume that, whether naturally or following chemical thinning, only the fruitlets with the greater sink capacity or the best supply in nutrients are maintained on the corymbs.

Commonly in apple, the central fruitlet develops earlier, as it originates from an earlier (1–3 d) flowering event. Thus, it naturally exerts a correlative dominance over the lateral fruits, making the latter weaker sinks and more inclined to abscise. However, unless treated, some cultivars, such as cv Ariane, are known to retain all their fruitlets, while others, like cv Granny Smith and cv Idared, have a tendency to self-abscise most lateral fruitlets. Thus, we hypothesize that the correlative dominance of central fruits observed in some cultivars may be due not only to an earlier flowering event but also to a better supply of sugar and nutrients through vascular tissues during the first weeks of development.

The vascular system is an elaborate network of conducting tissues that interconnects all plant organs. Its development is initiated by the formation of provascular cells that further develop into procambium, from which both conducting tissues are eventually differentiated (Steeves and Sussex, 1989). In most gymnosperms and dicots, vascular bundles are organized as a ring in the stem, with xylem located in the center and phloem surrounding it, whereas in monocots, vascular bundles are usually organized in an amphivasal fashion (i.e. the xylem surrounds the phloem; Zhong et al., 1999).

In past decades, mechanisms determining vascular pattern formation in model species have been intensively studied using physiological, biochemical, and molecular approaches. It has been shown that the induction of vascular differentiation is mainly controlled by auxin (Aloni et al., 2000). In normal development, auxin is synthesized in shoot apical tissues and is actively transported toward the base of the plant (Sachs, 1981). Besides auxin, evidence suggests a role for sterols (Szekeres et al., 1996; Yamamoto et al., 1997), small peptides (Casson et al., 2002), and cytokinin (Mähönen et al., 2000) in promoting vascular differentiation.

Application of molecular genetic tools accelerated the identification of genes involved in vascular development, especially in Arabidopsis. These include particularly an class III homeodomain-leucine zipper (HD-ZIP III) gene family composed of five members: Arabidopsis B15 (ATHB15), ATHB8, PHAVOLUTA, PHABULOSA, and REVOLUTA. Unlike the others, ATHB15 and ATHB8 are predominantly expressed in vascular tissues, suggesting a specific role in vascular development (Baima et al., 1995, 2001; Ohashi-Ito and Fukuda, 2003; Kim et al., 2005).

Until now, most studies on apple fruitlet abscission have been directed toward the identification of genes and signaling pathways activated in fruit cortex and seeds following shading and the application of hormonal (ethylene) or chemical thinner (benzyladenine) treatments (Zhou et al., 2008; Dal Cin et al., 2009; Botton et al., 2011). Recently, a study aimed at characterizing the genetic determinism of apple fruitlet self-thinning in a segregating population was undertaken, and several quantitative trait loci controlling this trait were identified (Celton et al., 2014b). In this study, the self-thinning capacity of the apple tree hybrid X3177 (obtained from the Institut National de la Recherche Agronomique) was characterized from the tree scale to the molecular level. First, fruit drop dynamics was investigated at the tree and corymb scale. Second, in order to understand the mechanisms controlling the acquisition of central fruit dominance leading to lateral fruitlet abscission, a histological study of the central and L1 flower/fruitlet pedicels was conducted from the phenological stage E2 (tight cluster, when the sepal lets the petals appear on the central flower) to fruit drop. Global transcriptional profiles of contrasting pedicels at four developmental stages were then assessed. Third, a histological study was conducted to characterize the development of lateral fruit AZs following the acquisition of central fruit dominance. Global transcriptional profiles of activated AZs were then compared with preformed AZs of persisting central fruits. Finally, we propose a model based on candidate genes and histological results to explain (1) the naturally exacerbated dominance of X3177 central fruitlets over lateral ones and (2) the activation and development of AZ in lateral fruitlet pedicels.

RESULTS

Fruit Drop Dynamics

The natural abscission maximum intensity for both X3177 trees was reached between 42 and 58 d after F1 stage, with a peak at 50 d (560°C cumulated temperature; Fig. 1). At the end of the experiment, the total fruitlet drop was 1,429 and 895 for the two biological replicates. Following this natural drop, the fruit category retained by the corymbs was evaluated. Our results show that a majority of corymbs retained only one fruit (except corymbs located at the distal end of branches) and that in 66% of cases, this fruit is the central fruit. The other 34% are composed of L3 fruits.

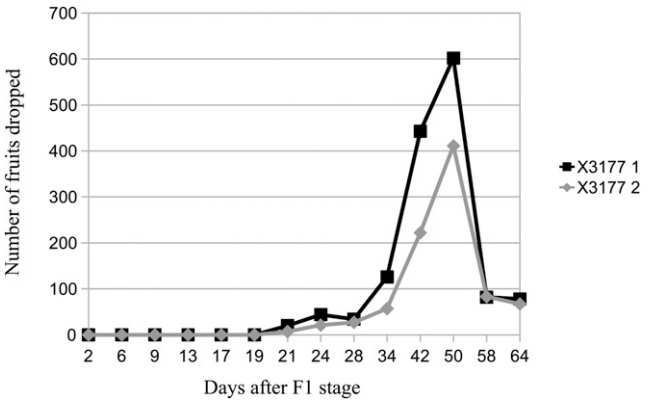

Figure 1. Fruit drop dynamics at the tree scale for both X3177 trees, expressed as the number of fruitlets dropped per tree following F1 stage (central flower opened).

The drop potential of the fruits was investigated by evaluating their order of abscission relative to their categories using the 30 hand-pollinated corymbs. The analysis revealed that 70% of corymbs retained at least one fruit. Fruit drop dynamics was similar to that found at the tree scale, with most fruits abscising 42 to 50 d after pollination (DAP). Although L1 fruits tended to abscise earlier than others, lateral fruit abscission did not occur in any particular order (Supplemental Fig. S1) or upon reaching any specific size (Supplemental Fig. S2). However, we found that the drop potential of each lateral fruit was corymb specific. We showed that lateral fruits were likely to abscise if their volume or growth rate was not maintained above about 50% of the volume and rate of the fastest growing fruit of the corymb (Supplemental Fig. S3).

To understand the sequence of events leading to lateral fruit cessation of growth and shedding in X3177, L1 and central fruit diameters were measured and compared following pollination. A similar analysis was performed on corymbs from the nonshedding cv Ariane. Measures indicated that for X3177 in 2011, the central fruit followed a linear increase in diameter from 6 to 22 DAP, while the L1 fruit stopped growing about 12 to 15 DAP (Fig. 2). From 12 to 22 DAP, L1 fruit diameter did not change significantly. On the contrary, for cv Ariane, both central and L1 fruits followed a linear growth throughout the first 22 DAP, with the central fruit having a larger diameter compared with the L1 fruit. The first L1 fruit abscissions were observed 22 to 23 DAP for X3177.

Vascular Development in X3177 Fruit Pedicels

To investigate the origin of the dominance of the central fruitlet over the lateral ones, we collected pedicels of central and L1 fruits at several time points during the course of flower and fruitlet development. Observations of cross sections of pedicels indicated the systematic presence of two to five additional amphivasal

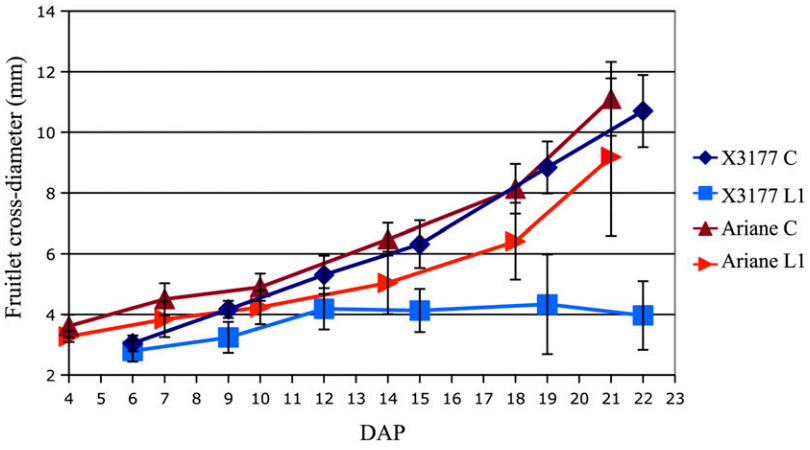

Figure 2. Central (C) and L1 fruitlet mean cross-diameter kinetics of X3177 and cv Ariane trees in 2011, from 4 to 22 DAP. Error bars represent SD. [See online article for color version of this figure.]

vascular bundles in the pith of central pedicels of X3177 fruits (Fig. 3A1). These additional vascular bundles were not present in L1 pedicels of X3177 (Fig. 3A2). Additional vascular bundles were not observed in central (Fig. 3A3) and L1 (Fig. 3A4) pedicels of cv Ariane. Further analyses indicated that vascular bundles were also absent from pedicels of L2 and L3 fruits of X3177.

To survey the timing of amphivasal vascular bundle development, we prepared free-hand sections from central pedicels harvested at different developmental stages. We found that vascular bundles were present within the central pedicel pith of X3177 as early as stage E2, up to 10 d before F1 stage (Fig. 3B1). We next investigated the origin of the formation of these additional vascular bundles by preparing serial cross sections of central pedicels, starting from the base of the fruitlet. We found that at the base of the fruit, the phloem tissue composing the ring-shaped bundles outgrew and abnormally penetrated into the pith (Fig. 3B2). These clusters of cells later rearranged themselves into amphivasal bundles farther down the pedicels. Unlike collateral bundles, X3177 amphivasal vascular bundles appeared to be mainly composed of phloem, with very few xylem cells present on the outer side of the bundles (Fig. 3C). Additional amphivasal bundles varied in size from a few cells to several hundred cells, organized in stratified way (Fig. 3C2). At the center of each bundle (enclosed by the phloem), a cluster of compressed or sclerified cells with thick walls was observed (Fig. 3C2).

In order to determine whether the self-thinning characteristic is associated with additional amphivasal bundles, we studied the cosegregation of these traits in 18 individuals descended from X3177. We found that none of the five individuals classified as "several fruits per corymb" had these bundles (in central and lateral fruits), while nine (69%) of the 13 individuals classified as "one fruit per corymb" had additional amphivasal bundles in the pith of their central pedicel (Table I). This result indicates that in our experimental conditions, the final number of fruits brought to maturity on the corymbs is associated with the presence of additional amphivasal bundles in the pith of central fruit pedicels.

Measurement of Central and Lateral Pedicel Sugar Content

The development of additional conducting vessels may allow the central fruit to be better supplied with sugars and nutrients from the tree. To test this hypothesis, we collected pedicels from central and L1 fruitlets at three time points in 2013 and measured the different sugar concentrations. Sorbitol, Glc, Fru, and Suc levels were assessed in all samples at 12, 15, and 20 DAP. As shown in Figure 4A, both central and L1 fruitlets are still growing at 12 DAP, although central fruitlet diameter is already significantly larger than L1 fruitlet diameter. At 15 DAP, L1 fruitlets seem to have reached a maximum and enter a phase in which they stop evolving. Finally, at 20 DAP, L1 fruitlet diameter starts decreasing ($P < 0.05$), probably due to dehydration, while central fruit diameter keeps increasing.

In the majority of the samples tested (except L1 at 20 DAP), the most concentrated sugar was sorbitol, followed by Glc, Suc, and Fru. Significant variations between central and L1 pedicels were found throughout the experiment for sorbitol (Fig. 4, B–D). Thus, a correlation between the abscission potential of the fruit and the concentration of sorbitol in its pedicel was established. Concerning Glc, a significant difference between central and L1 pedicels was found at 20 DAP. A significant difference was found for Fru concentration at 15 DAP. Finally, significant differences between central and L1 pedicels were found at 12 and 20 DAP for Suc.

This difference in sugar supply, and particularly sorbitol, may contribute to making the central fruit a major sink while making the lateral fruits weaker and, in time, more prone to abscise.

Differential Gene Expression Analysis between Central and L1 Pedicels

To identify genes whose expression pattern matched with a potential role in additional amphivasal vascular tissue development, global transcript expression

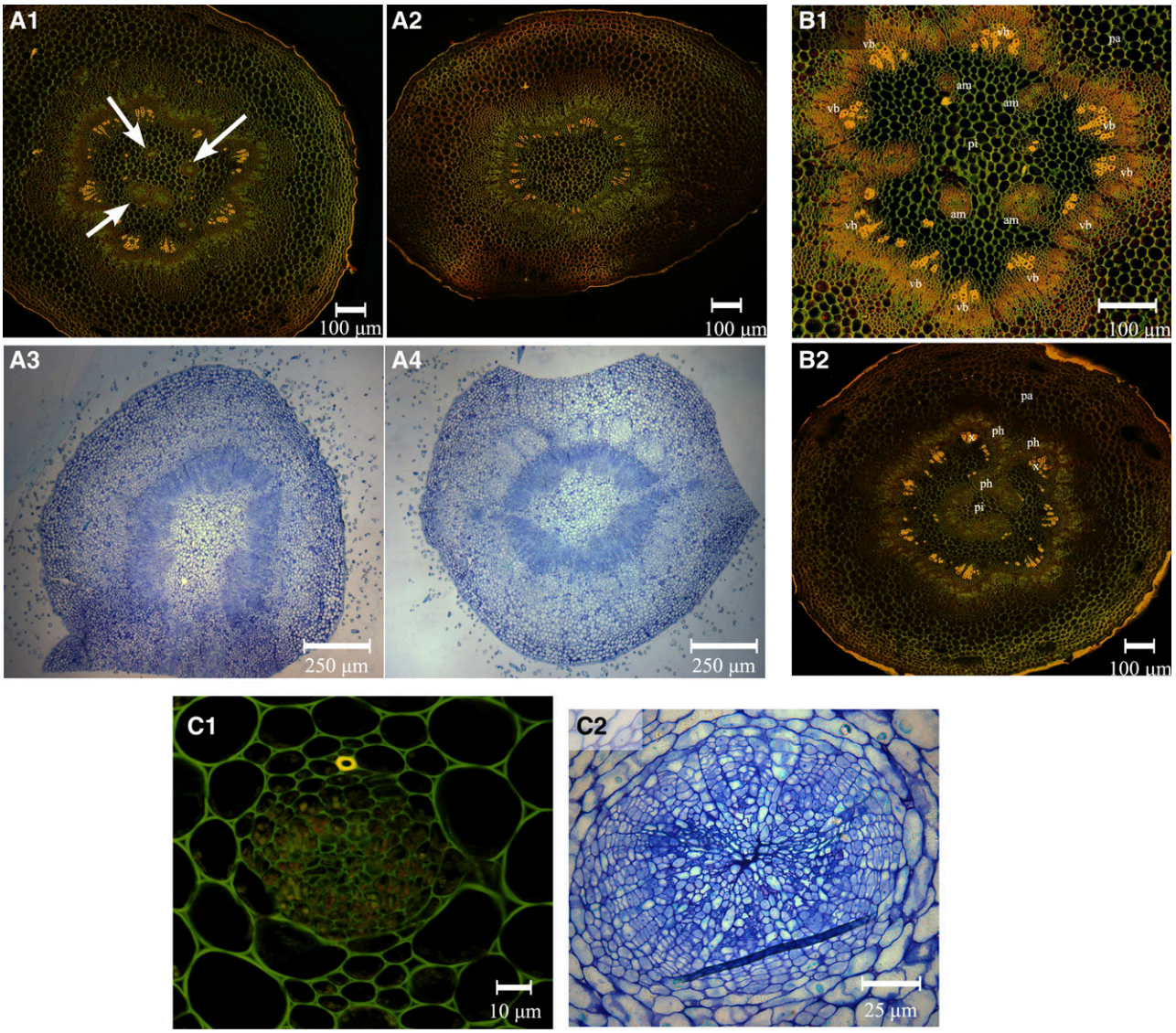

Figure 3. Vascular patterns in central and L1 fruitlet stems of the apple hybrid X3177 and cv Ariane. A1 and A2, Pedicel cross section of X3177 central (A1) and L1 (A2) fruitlets 8 DAP, stained with acridine orange. Arrows indicate the positions of additional amphivasal bundles in the pith of central pedicels. A3 and A4, Pedicel cross section of cv Ariane central (A3) and L1 (A4) fruitlets 7 DAP, stained with toluidine blue. No amphivasal vascular bundles are observed in cv Ariane central pedicels. B1, Cross section of X3177 central flower pedicel at stage E2 (tight cluster, when the sepal lets the petals appear on central flower), stained with acridine orange. Surrounded by parenchyma (pa), vascular bundles (vb) are arranged in a ring pattern, with additional amphivasal bundles (am) located in the pith (pi). B2, Cross section of X3177 central pedicel cut at the base of the flower at stage E2, stained with acridine orange. Phloem (ph) tissues seem to abnormally penetrate into the pith of the pedicel. x, Xylem. C1, Cross section of amphivasal vascular bundle in the pith of the central pedicel of X3177 at the F1 stage (central flower open), stained with acridine orange. Cells are not yet organized, and only a single lignified cell is observed (in yellow). C2, Cross section of X3177 amphivasal vascular bundle in the pith of the central pedicel of X3177 19 DAP, stained with toluidine blue. Cells composing this bundle are organized in stratified layers, with compressed or sclerified cells at the center. The scale is represented by a bar at the bottom of each image.

profiling was performed using the ARyANE microarray chip at four time points (E2, F1, 6 DAP, and 12 DAP), a period spanning the earliest phase of amphivasal vascular bundle development to the L1 fruit growth arrest.

Over this period, 6,327 transcripts showed statistically significant ($P < 0.05$) expression changes in at least one time point, including 2,005 with a log ratio above 1. Of these transcripts, 253 were down-regulated (ratio > -1 log) and 235 were up-regulated (ratio > 1 log) in L1 pedicels at stage E2; 660 were down-regulated and 955 were up-regulated in L1 pedicels at stage F1; 120 were down-regulated and 156 were

Table I. *Identification of additional amphivasal bundles in the pith of fruit pedicels from individuals with contrasting phenotypes*

For each individual, the cross from which it originates is indicated as well as the number of amphivasal bundles observed in the pith of the fruit pedicels. The average number of fruits brought to maturity per corymb is indicated in the right column.

Individual	Fruit Position[a]	Cross[b]	No. of Amphivasal Bundles	No. of Fruits per Corymb
G37	C	cv Generos × **X6681**	4	1
H85	C	X3259 × **X3263**	1	1
H94	C	X3259 × **X3263**	1	1
H102	C	X3259 × **X3263**	2	1
I67	C	X3259 × **X3263**	1	1
I79	C	X3259 × **X3263**	1	1
I104	C	X3259 × **X3263**	5	1
V10	C	X3259 × **X3263**	5	1
V82	C	X3259 × **X3263**	1	1
V92	C	X3259 × **X3263**	0	1
W103	C	X3259 × **X3263**	0	1
M18	C	X7940 × **X6681**	0	1
M19	C	X7940 × **X6681**	0	1
	C	X7940 × **X6681**	0	2–4
M91	L	X7940 × **X6681**	0	
	C	X7940 × **X6681**	0	2–4
M31	L	X7940 × **X6681**	0	
	C	X7940 × **X6681**	0	2–4
M1	L	X7940 × **X6681**	0	
	C	X3259 × **X3263**	0	2–4
I34	L	X3259 × **X3263**	0	
	C	X3259 × **X3263**	0	2–4
H95	L	X3259 × **X3263**	0	

[a]C, Central fruit; L, lateral fruit. [b]Hybrids indicated in boldface originate from a cross with X3177.

up-regulated in L1 pedicels at 6 DAP; and finally, 55 were down-regulated and 194 were up-regulated in L1 pedicels at 12 DAP.

More genes were differentially expressed at stages E2 and F1, which may indicate that morphological differences resulting from differential gene expression between central and L1 pedicels may develop during these two stages.

Time points and differentially expressed genes were grouped using K-means clustering (MapMan; Supplemental Table S1). Based on the similarity of the kinetic expression pattern, genes were divided into six clusters (Fig. 5). Most clusters reflected either up- or down-regulation at two to three time points.

Our analysis reveals that the transcriptional activity of genes involved in cell wall modification, response to stress, lipid metabolism, and lignin synthesis is significantly up-regulated in L1 pedicels at an early stage in their development. In central pedicels, the overexpression of genes associated with vascular tissues, and more particularly with phloem tissues, may be related to the development of additional amphivasal vascular bundles and to a better supply of nutrients to the central fruit (Fig. 5). This indicates that the mechanisms ultimately leading to the shedding of lateral fruitlets are activated very early during corymb development and that modifications in gene expression progressively lead to nutritional shortages and activation of the lateral fruitlet abscission process.

For microarray data validation, reverse transcription-quantitative PCR (RT-qPCR) experiments were performed on a subset of selected genes and revealed similar expression patterns and strong correlations (Spearman correlation coefficient = 0.81; Supplemental Table S2).

To further study the mechanisms involved in amphivasal bundle formation, we investigated the expression patterns of the HD-ZIP homeobox genes ATHB8 and ATHB15. We found that the differentiation-promoting transcription factor of the vascular meristems of ATHB8 was slightly up-regulated at 6 DAP (ratio of −0.73; $P = 0.07$). To validate the overexpression of this transcription factor, we performed RT-qPCR analysis and found a ratio of −1.75 at 6 DAP. In the mean time, the negative regulator of vascular development ATHB15 was up-regulated at stage F1 in L1 pedicels (ratio of 0.72; $P = 0.005$). In addition, our microarray results indicated a down-regulation of miR166 (ratio of −0.72; $P = 0.006$), a negative regulator of ATHB15, in L1 pedicels at stage F1.

Dynamics of AZ Development in X3177 Lateral Pedicels

To investigate the sequence of events leading to AZ activation and development following fruit growth arrest, longitudinal sections of X3177 central and L1 pedicels were harvested at 14, 17, and 21 DAP. Observation

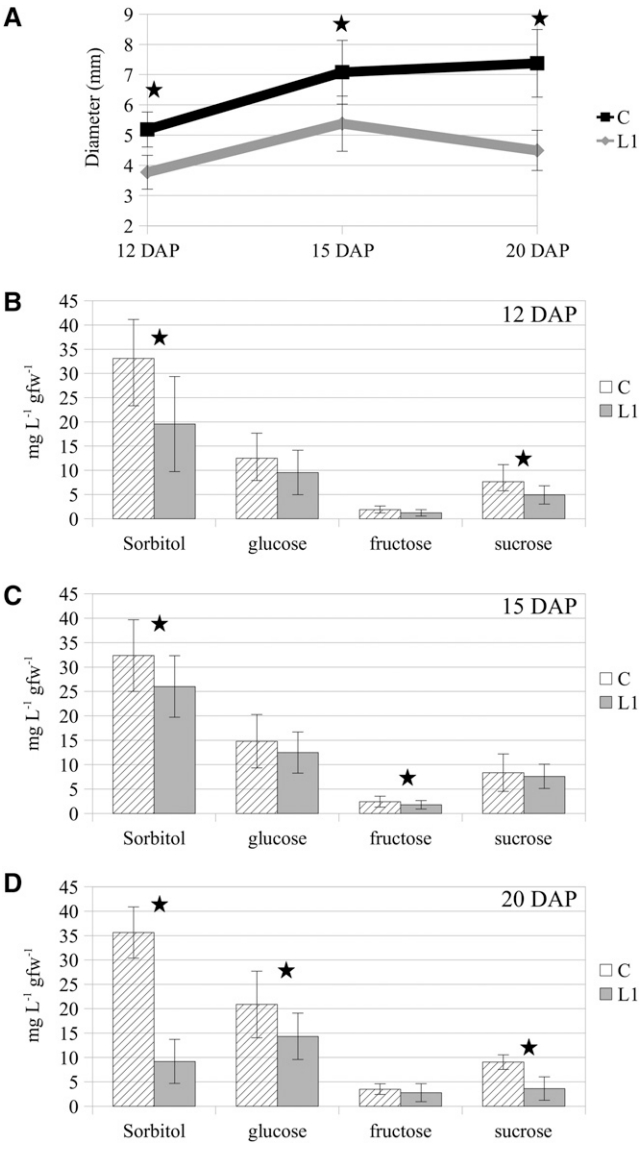

Figure 4. A, L1 and central (C) diameters of selected hand-pollinated fruits at 12, 15, and 20 DAP of the apple hybrid X3177 in 2013. B to D, Sugar concentrations in central and L1 pedicels at three time points: 12 DAP (B), 15 DAP (C), and 20 DAP (D). Error bars represent SD. Statistically significant differences between the central and L1 pedicels as identified by Student's *t* test are indicated by stars ($P < 0.05$). gfw, Grams fresh weight.

of potential AZs from central pedicels did not reveal any difference among the three time points (Fig. 6A). For L1 pedicel AZs, three phases were identified. The first phase (14 DAP; Fig. 6B1) corresponds to a phase during which the AZ is preformed and located at the limit between large parenchyma cells on the pedicel side and smaller cells on the bourse side, above the invagination. This stage is similar to that found in the central pedicel. During the second phase (17 DAP; Fig. 6B2), which corresponds to the activation of the AZ, dividing cells were observed (Fig. 6C) in a region located above the invagination zone. In the third phase (Fig. 6B3), the AZ was visible and composed of a layer of 15 to 20 cells. Stratified cells derived from the cell division phase were observed (Fig. 6, D1 and D3). At this point, the AZ can be divided into two sections: on the pedicel side, cell walls appear lignified and more voluminous, while on the bourse side, the stratified cell wall appears mainly composed of cellulose, with potential suberin deposition on the inner face of primary cell walls (Fig. 6D1). Further observation by scanning electron microscopy indicates the formation of a large depression formed by the degradation of cell walls at the interface between the two sections described above (Fig. 6D2).

To gain a global view of the transcriptional regulation mechanisms associated with the activation and development of the AZ in the L1 fruitlets, we set up a transcriptome analysis using the ARyANE microarray chip.

Differential Expression of Genes Involved in AZ Activation and Development in L1 Pedicels

To identify the genes involved in the activation and development phases of X3177 pedicel AZ, expression profiling was performed on central and L1 AZ tissues corresponding to the three phases observed in our histological studies (14, 17, and 21 DAP). Over these three time points, we identified 3,625 significantly differentially expressed genes ($P < 0.01$; log ratio > 1). The majority of these genes were found during the third phase of AZ development (21 DAP), with 2,185 genes up-regulated and 381 genes down-regulated in L1 AZ. During the activation phase (17 DAP), 688 genes were found to be overexpressed in L1 AZ, while 814 were identified as down-regulated. Finally, 501 genes were up-regulated in L1 AZ during the first phase (14 DAP), while only 43 were identified as down-regulated.

Based on the similarity of the kinetic expression pattern, genes were divided into nine clusters: up-regulated, unchanged, or down-regulated for each time point and biological repeat (Supplemental Table S3). This analysis allowed us to attribute each pattern of expression to one or several of the phases of AZ activation and development (Fig. 7).

Our analysis showed a significant up-regulation of genes involved in cell wall modification and degradation (glycosyl hydrolases, hydrolases, polygalacturonases, laccase, and pectinesterase), ethylene response factors, and GA oxidase in L1 pedicels during the last phases of AZ development. In addition, we identified many genes up-regulated in L1 AZ with sequence homology to genes involved in defense response mechanisms, dehydration, senescence, and suberin and lignin biosynthesis. We also identified genes significantly down-regulated in L1 AZ, particularly during the

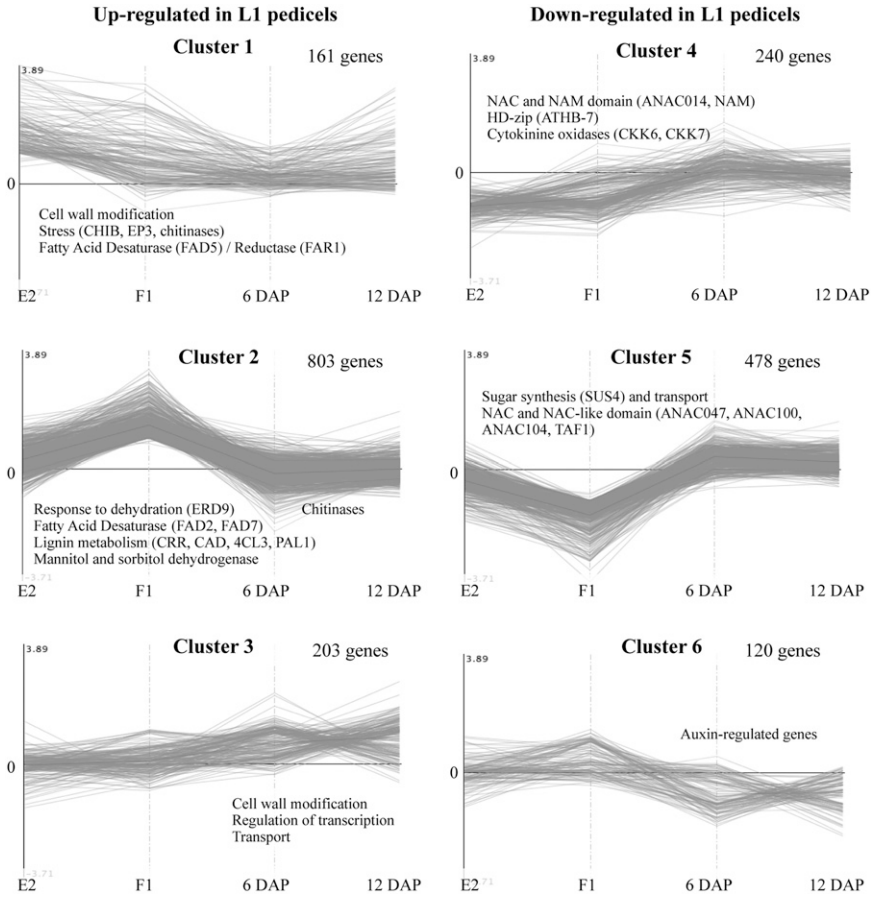

Figure 5. K-means clustering of significantly differentially expressed genes between central and L1 pedicels at four developmental stages (E2, F1, 6 DAP, and 12 DAP). The left column represents clusters of genes up-regulated in L1 at one or more developmental stages. The right column represents clusters of genes down-regulated in L1 at one or more developmental stages. The number of genes in each cluster is shown next to the cluster number. Names of selected genes or gene families are indicated in each cluster.

activation phase (17 DAP), including auxin response factors and plant-specific pin-formed proteins, as well as genes involved in Suc synthesis and transport.

DISCUSSION

The hybrid X3177 is a unique model system for studying natural lateral fruitlet self-thinning in apple. Despite the characterization of the genetic determinism of fruitlet self-thinning (Celton et al., 2014b), the selection of elite cultivars exhibiting this characteristic remains largely empirical. The quasi-systematic acquisition of dominance of central fruitlets over the lateral ones allows the setting up of experimental designs aimed at deciphering the processes involved in the natural acquisition of this dominance and the activation of fruitlet AZ. Previous studies carried out by Dal Cin et al. (2009), Botton et al. (2011), and Zhu et al. (2011) had addressed similar issues. However, those studies were performed on commercial cultivars using thinning chemicals able to magnify the abscission potential and selectively induce fruit drop. The focus of our research here was to characterize the self-thinning capacity of the apple tree hybrid X3177 from the tree scale to the molecular level.

Lateral Fruitlet Drop Occurs within 2 Months after F1

In spring, a competition for storage assimilate reallocation exists between the vegetative and reproductive parts of the tree, among corymbs, and among fruits of the same corymb. Part of the model devised for apple fruitlet abscission stipulates that, where a nutritional stress is established, the weaker sinks, represented by the smallest growing fruitlets, abscise, thus generating the physiological drop. Our data suggest that in X3177, this phenomenon is genetically exacerbated. In fact, in the absence of external perturbations, a majority of corymbs retain only one fruit, mostly the central fruit and to a lower extent the L3, while the L2 and L1 all undergo shedding. Therefore, we identified an increasing gradient of abscission potentials, starting from the L1 toward the central fruit, as described previously by Botton et al. (2011). However, no particular order in lateral fruit drop was observed. Unlike the findings of Botton et al. (2011) and Eccher et al. (2013) for cv Golden Delicious, the fruit drop dynamics appeared monophasic, with most fruitlets abscising 50 DAP for both biological replicates. This divergence in fruit drop dynamics indicates that trees may have developed different strategies to regulate their fruit overload.

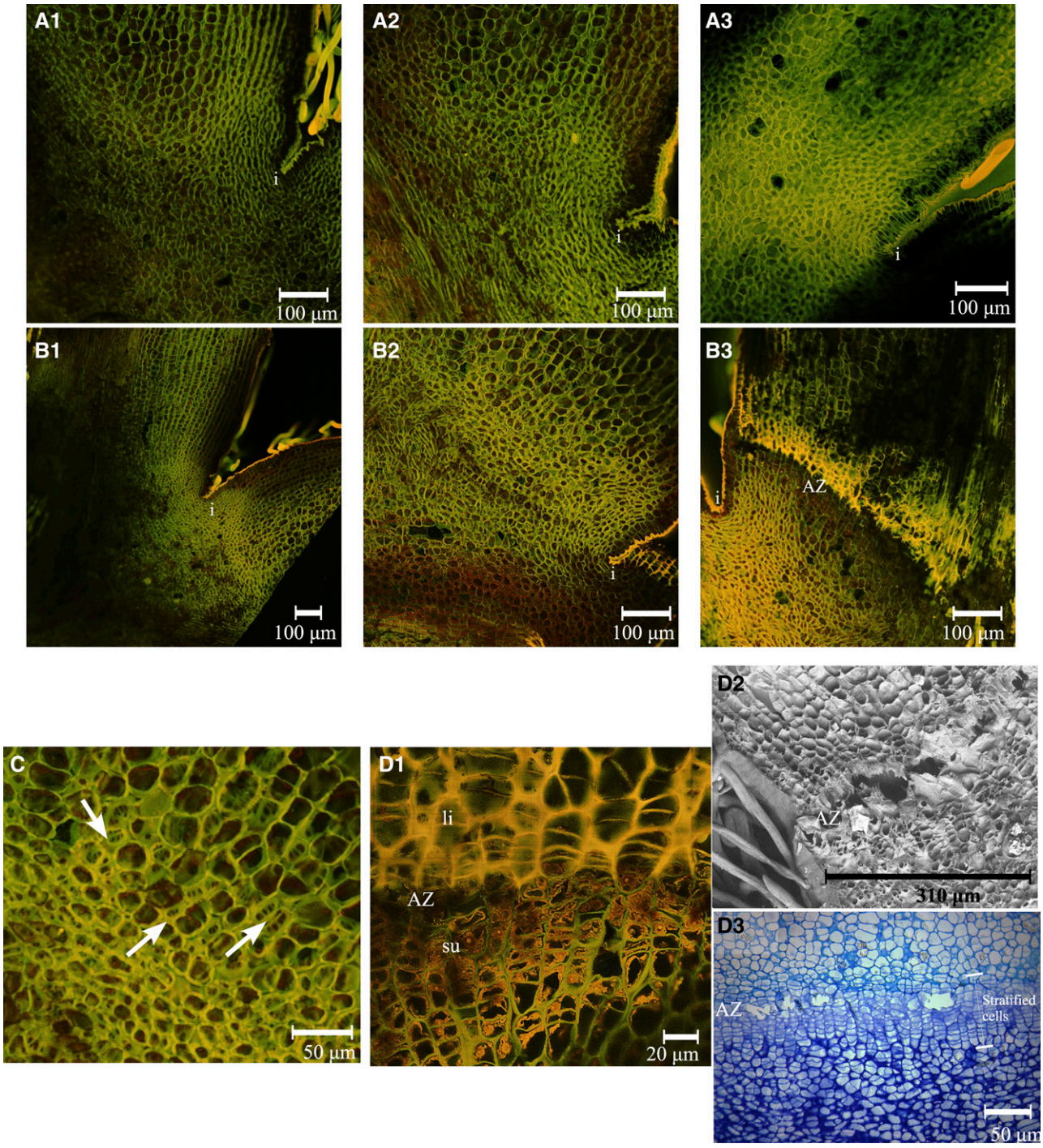

Figure 6. AZ development at the base of X3177 pedicels. A, Development of AZ in central pedicels at 14 DAP (A1), 17 DAP (A2), and 21 DAP (A3), stained with acridine orange. The AZ did not develop in the course of these three dates. i, Invagination. B, Development of AZ in L1 pedicels at 14 DAP (B1), 17 DAP (B2), and 21 DAP (B3), stained with acridine orange. The development of an AZ, represented by layers of different colored cells, is clear at 21 DAP. C, Closeup view of the AZ in L1 pedicels at 17 DAP, stained with acridine orange. Arrows indicate the positions of dividing cells. D, Closeup views of the AZ in L1 pedicels at 21 DAP. D1, Pedicel section stained with acridine orange. The AZ is divided in two; the top section (fruitlet side) is composed of large stratified cells with lignified cell walls (li), and the bottom section (bourse side) is composed of smaller stratified cells with possible suberin deposition on the inner face of primary cell walls (su). D2, Scanning electron microscopy of AZ in L1 pedicels at 21 DAP. Cell wall and middle lamella degradation is observed in the separation layer. D3, Pedicel stained with toluidine blue. The stratified cells composing the AZ and the separation layer can be observed. The scale is represented by a bar at the bottom of each image.

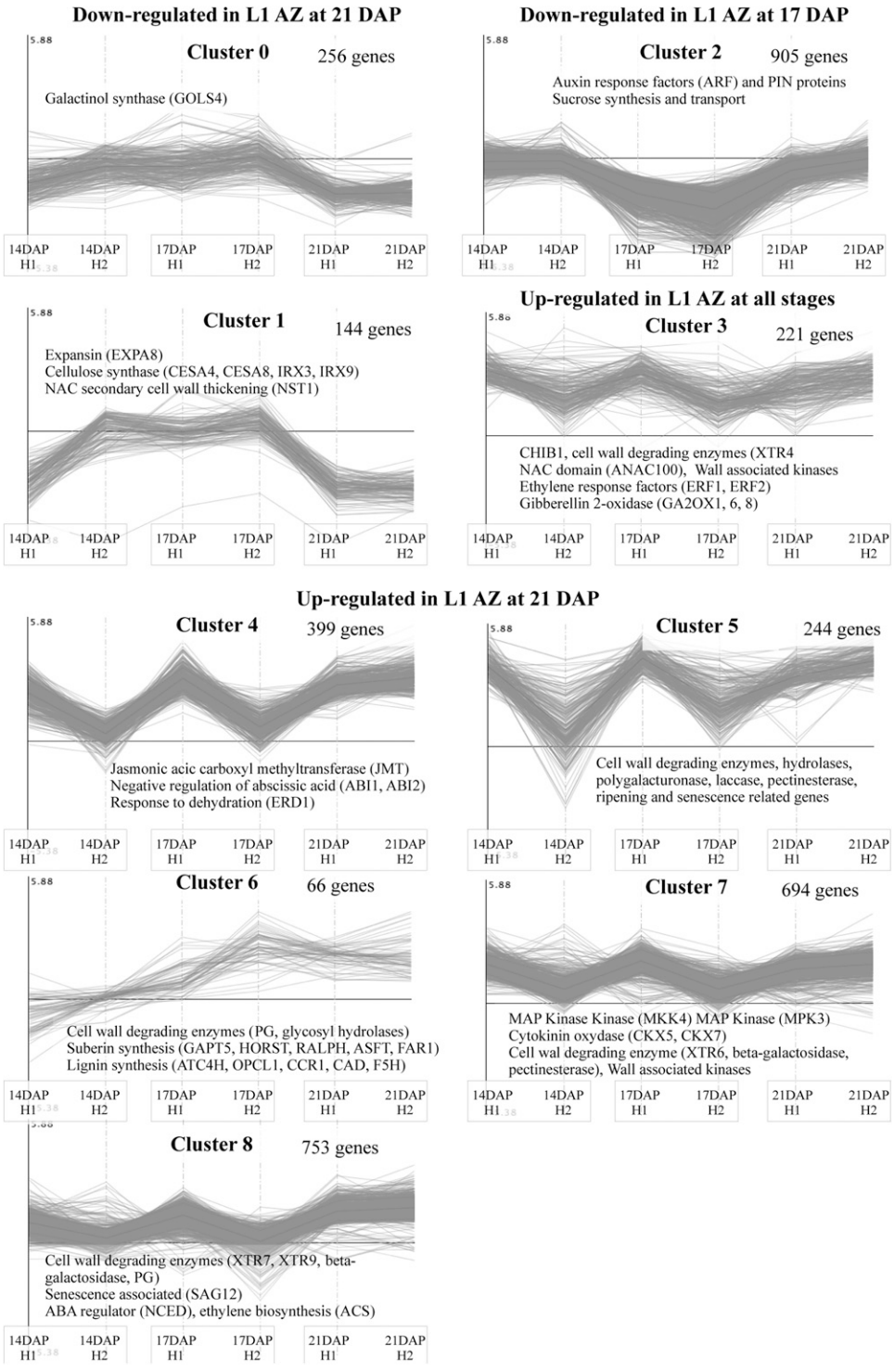

Figure 7. K-means clustering of significantly differentially expressed genes between central and L1 AZ at three developmental stages (14, 17, and 21 DAP) for the two X3177 biological replicates (H1 and H2). Clusters have been regrouped according to their profiles. The number of genes in each cluster is shown next to the cluster number. Names of selected genes or gene families are indicated in each cluster.

Central X3177 Fruit Pedicels Contain Additional Amphivasal Vascular Bundles in Their Pith

To understand the acquisition of central fruit dominance over lateral ones in the first weeks after F1 stage, we hypothesized that these central fruits were better supplied in sugars and nutrients through vascular tissues, and we investigated potential differences in vascular tissue development between central and L1 fruitlet pedicels.

Our histological data suggest the systematic presence of additional amphivasal vascular bundles of various sizes in the pith of X3177 central pedicels in addition to the vascular bundles being arranged in a ring pattern. Amphivasal bundles were observed early in the development of the inflorescence (stage E2; i.e.

several days before flowering). As described by Dražeta et al. (2004), we found that vessel formation, and thus the hydraulic conductance of the pedicel, starts before flowering. The timing and dynamics of additional amphivasal bundle differentiation suggest that they may be active before pollination.

To confirm the histological observations, our differential gene expression among X3177 pedicels allowed us to identify a trend toward a down-regulation of genes potentially involved in vascular tissue differentiation in L1 pedicels in the early stages of development. Among them, we identified multiple NAC (for no apical meristem, ATAF1/2, cup-shaped cotyledons2) family proteins. The NAC proteins constitute one of the largest plant-specific families of transcription factors (Riechmann et al., 2000; Ooka et al., 2003). These proteins have been implicated in diverse processes, such as developmental programs, including secondary cell wall biosynthesis in poplar (*Populus* spp.; Zhong et al., 2011), shoot apical meristem formation and development (Aida et al., 1999), defense, and abiotic stress responses (Olsen et al., 2005). Expression analyses have also supported the involvement of NAC genes in flower development and reproduction in response to hormones, including auxin, in the acquisition of pluripotentiality (Avivi et al., 2004) and the establishment/maintenance of stem cell lineage in plants (Duval et al., 2002). Zhao et al. (2005) identified a variety of NAC domain proteins involved in vascular tissue differentiation. In our study, we found several genes encoding NAC domain transcription factor up-regulated in the pedicel of central fruits (ANAC014; Fig. 8), indicating that these genes might contribute to an increased vascular development in the central pedicel in the early developmental stages E2 and F1.

As mentioned previously, auxin and cytokinin are important regulators of xylem cell differentiation. Among the transcripts overexpressed in the central pedicel, we identified two genes encoding cytokinin synthases (homologous to At3g63100 and At5g19040) previously reported to be associated with phloem development (Takei et al., 2004). In addition, we identified two genes homologous to cytokinin oxidase (cytokinin oxidase6 and cytokinin oxidase7), involved in the

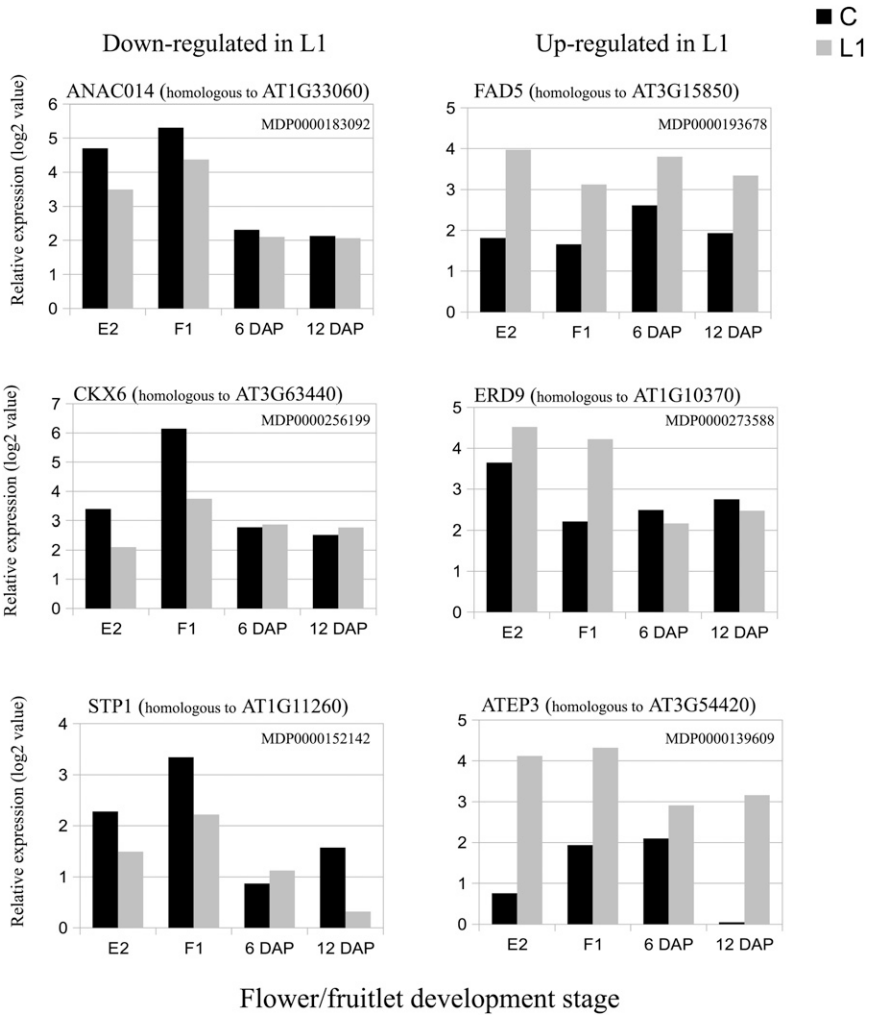

Figure 8. Kinetics of the expression values of genes differentially expressed between central (C) and L1 X3177 apple pedicels as determined by microarray analysis at four developmental stages (E2, F1, 6 DAP, and 12 DAP). The left column shows expression values (log values) of genes significantly down-regulated in L1 compared with central pedicel sections. The right column shows expression values (log values) of genes significantly up-regulated in L1 compared with central pedicel sections. The array data were normalized with the lowess method. Normalized intensities (i.e. expression levels) were then subtracted from the background.

degradation of cytokinines, overexpressed in L1 pedicel fruitlets at stages E2 and F1 (Fig. 8).

Our analysis of genotypes derived from X3177 suggests that, over these extreme individuals and in our environmental conditions, the presence of amphivasal bundles in the pith of pedicels of fruits brought to maturity is associated with the self-thinning character. Although this analysis was performed on a limited number of individuals, it demonstrates that the presence of amphivasal bundles in the pith of pedicels is heritable. At this point, several questions remain open. Are the amphivasal bundles always located in the central pedicel, or can they be found in lateral pedicels? If all pedicels of the corymb have amphivasal bundles, the central fruit dominance may not be exacerbated, so what is the tree bearing behavior then? Further investigation should focus on the particular role of these additional bundles and determine how the expression of this characteristic is controlled in a dedicated segregating population, such as the one used by Celton et al. (2014b). Such study may confirm whether the self-thinning trait is associated with the presence of amphivasal bundles in the central pedicel only.

The common arrangement of vascular tissues in most dicots is collateral, where the xylem is located on the inner side and the phloem on the outer side of the bundle, the latter being arranged collectively in a ring pattern. Even though other vascular patterns have evolved in some dicots, the ring-type pattern has been mostly conserved during the evolution of dicot plants. Little is known about the mechanisms underlying the development of vascular patterns, and to date, very few mutants have been identified with global alteration of vascular arrangement. One such Arabidopsis mutant, *amphivasal vascular bundle1* (*avb1*), was identified by Zhong et al. (1999). This plant presents a dramatic alteration of the arrangement of vascular tissues, with vascular bundles arranged in an amphivasal fashion (i.e. with the xylem completely surrounding the phloem). These amphivasal bundles were found to abnormally penetrate into the pith and did not disrupt the auxin polar transport activity in inflorescence stems.

As for the *avb1* mutant, X3177 amphivasal vascular bundles were found in the pith of stems without disruption of the ring-like pattern of vascular bundles. Further analysis showed that amphivasal bundles arise from an overproduction of phloem at the base of the future fruit. Unlike in the *avb1* mutant, the amphivasal bundles were mostly composed of phloem tissue, with very few xylem cells on the outside. As in *avb1*, the arrangement of phloem cells was organized, and sclerified cells were identified at the center of the bundles.

HD-ZIP genes and their related microRNAs regulate critical aspects of plant development, including vascular development, and represent ancient gene families conserved in all tracheophytes (Schuetz et al., 2013). The microRNAs miR165 and miR166 have been shown to directly regulate HD-ZIP patterning (Kim et al., 2005). These microRNAs are known to be present within the phloem, and their overexpression leads to enhanced degradation of HD-ZIP transcripts, leading to a phenotype corresponding to that of an HD-ZIP loss-of-function mutant (Kim et al., 2005; Zhou et al., 2007). Furthermore, dominant HD-ZIP mutants have been found to display amphivasal phenotypes. As shown by Baima et al. (2001), the HD-ZIP gene ATHB8 is induced by auxin and promotes procambial/cambial cell differentiation into xylem tissue. We found an apple homolog of ATHB8 to be underexpressed in L1 pedicels 6 DAP, which may indicate a lower auxin production in the developing lateral fruit and a possible decrease in lateral vascular development compared with the central pedicel. ATHB15 is important for vascular development and is responsible for its negative regulation, independently of auxin (Kim et al., 2005). Kim et al. (2005) hypothesize that miR166/miR165 could act as a modulator to balance ATHB15 and ATHB8 functions during vascular development. In our analysis of vascular development of apple pedicels, we found miR166 to be down-regulated in L1 pedicels, with a corresponding enhanced expression of an apple homolog of ATHB15 at the E2 stage. Although the log ratios are below 1, they remain significant and indicate an increased negative regulation of vascular tissue biogenesis during a crucial stage in L1 pedicel development.

The Central Pedicel Sugar Concentration Is Higher Than That of the L1 Pedicels

The absence of amphivasal bundles in the pith of cv Ariane and other hybrid pedicels with several fruits per inflorescence (central and laterals) and in all the lateral pedicels of X3177 suggests that these bundles may have a role in the acquisition of the X3177 central fruit dominance by allowing an increased transport of sugars and nutrients to the young fruit. In our analysis, significant differences in sorbitol concentration between central and L1 pedicels were found at all time points investigated. In apple, sorbitol is the primary product of photosynthesis and is the major translocated form of carbon (Loescher et al., 1982). The increased sorbitol concentration in central pedicels is thus consistent with our hypothesis that central fruits profit from a better supply of sugars. This increased supply would allow the central fruit to develop at a faster rate, thus increasing further its sink strength. We believe that the increased supply of sugar to the central fruit is at least partly due to the presence of the additional amphivasal vascular bundles.

The increased expression of transcripts coding for enzymes involved in Suc metabolism may be expected in fast-growing organs, considering that the developing vascular system and fruitlet acts as a major carbon sink. In Arabidopsis, the up-regulation of genes involved in trehalose metabolism was reported in response to increased nitrate availability (Wang et al., 2003; Scheible et al., 2004). Sugars such as Glc and trehalose are also effective signal molecules and may have an essential role in many developmental processes (Rolland et al., 2006). In our experiment, trehalose-6-phosphatase, Man-6-P

reductase, and Suc synthase genes showed increased expression in the pedicels of central fruitlets. Furthermore, genes associated with sugar transport, such as *SUGAR TRANSPORTER1* (Fig. 8) and *POLYOL TRANSPORTER5*, were also identified as up-regulated in central pedicels during the early stages of development (E2 and F1) as well as 12 DAP. The up-regulation of genes associated with sugar metabolism and transport indicates that central pedicels may be better supplied from a very early stage of development.

Furthermore, sugar signaling is known to play a role in senescence regulation in a complex network resulting from biotic and abiotic stress (Wingler and Roitsch, 2008; Wingler et al., 2009). Thus, a decrease in sugar supply, as well as other nutrients, may have triggered a senescence process in lateral fruits. We found several genes differentially expressed that are associated with stress, dehydration, and senescence. Among them, we identified genes with sequence homology with the fatty acid desaturases FAD2, FAD5 (Fig. 8), and FAD7, which were up-regulated at all stages and are known to be regulated by adverse environmental factors (Zhang et al., 2012). Genes associated with dehydration were up-regulated in L1 pedicels, including *EARLY RESPONSIVE TO DEHYDRATION* (Fig. 8) at stages E2 and F1. This gene belongs to the glutathione *S*-transferase family and has been implicated in the response to dehydration in Arabidopsis (Kiyosue et al., 1993). Several genes homologous to Arabidopsis Extracellular Protein3 (chitinase class IV) were also constantly overexpressed in L1 pedicels (Fig. 8). Various factors were found to induce class IV chitinase expression, including leaf senescence in *Brassica napus* (Hanfrey et al., 1996), while in Arabidopsis and carrot (*Daucus carota*), Extracellular Protein3 is involved in the regulation of processes leading to programmed cell death (Passarinho et al., 2001). Overexpression of genes associated with lignin biosynthesis (Table II) also indicates that L1 pedicels may respond at an early stage to stresses caused by water and nutrient deficiency and may undergo lignification of their supporting tissues, which may further impair their capacity to convey water and nutrients (Ride, 1978) to the young fruit.

The identification of additional amphivasal vascular bundles in the pith of central pedicels of this apple hybrid is a unique example in dicot plants. We have shown that this phenotype develops in the early phases of pedicel growth, is localized only in the central pedicels of this hybrid, and confers the subtending fruit with an advantage in terms of sugar and nutrient supply. This extra supply allows the central fruit to develop faster than the lateral fruits, thus becoming the major sink within the corymb. Within a few days, the central fruit exerts a dominance over the lateral ones, which progressively stop growing and may enter into the senescence process. The differential gene expression analysis confirmed our histological observations and allowed us to identify several differentially expressed genes involved in vascular tissue development, sugar transport, and stress response. The histological and gene expression data presented here allow the development of novel hypotheses regarding the formation of the atypical additional amphivasal vascular bundles in the pith of central pedicels and its subsequent exacerbated dominance over the lateral fruitlets.

In order to gain a global view of the factors involved in fruitlet shedding, we next investigated lateral fruit AZ development following the acquisition of dominance of the central fruit.

The Stop of L1 Fruit Growth Occurs about 10 d before Abscission

In our analysis, 66% of the fruits remaining on the corymbs were central fruits, while in 34% of cases it was the L3. Thus, the central fruit acquisition of dominance was not systematic in our experimental conditions. In X3177, the central flower of the corymb opens 2 to 3 d before the L3 and other laterals. In 2013, the spring was unusually cold and wet during flowering, particularly at the F1 stage. This particular bad weather may have affected the pollination of central flowers, which may explain the rather high percentage of central fruitlet early drop. This is further confirmed by our analysis of fruit growth on particular corymbs. Our data show that L3 fruit acquired dominance only when the central fruit dropped early, within 200°d following F1. Furthermore, we found that lateral fruit abscission occurred when fruit growth rate and estimated volume were not maintained above a certain threshold. Lakso et al. (2001) estimated that threshold at about 60%, while in our experimental conditions, we found that fruits abscised if their volume was not maintained above 50% of the volume of the largest fruit in the corymb for about 200°d consecutively.

Our data indicate that fruit abscission did not occur immediately following lateral fruit cessation of growth. We showed that the AZ activation occurred 4 to 5 d after cessation of lateral fruitlet growth, with fruit drop occurring 5 to 6 d later. Thus, the AZ development is not synchronized with the stop of fruit growth, which confirms that the development of the AZ is not the factor controlling fruit self-thinning.

AZ Development Is Controlled by a Complex Gene Network

In our apple pedicels, the AZ cells were distinguishable from their neighboring cells in that they were smaller and located above the invagination. The physiological processes leading to cell separation were located within a narrow band of cells in which the separation layer developed. Our histological analysis of pedicel AZ development permitted the identification of three phases.

In the first phase, during which the AZ is already differentiated at the future site of detachment for both central and L1 fruits, we did not observe any histological

Table II. *Selection of differentially expressed genes in apple pedicels*

The gene identifier is reported along with the Arabidopsis gene homolog, a short annotation, and the pattern of expression at stages E2, F1, 6 DAP, and 12 DAP. The complete list and further details, are available in Supplemental Table S1. Log^2 rat, Log^2 ratio between lateral1 and central pedicel transcript expression value.

Apple Gene Identification	Arabidopsis Homolog	Annotation	Stage E2		Stage F1		6 DAP		12 DAP	
			log^2 rat	*P*	log^2 rat	*P*	log^2 rat	*P*	log^2 rat	*P*
Stress related										
MDP0000417095	AT3G12500	Basic chitinase (ATHCHIB)	1.73	7.01E-006	1.60	9.07E-005	0.50	4.51E-002	1.99	7.97E-004
MDP0000139609	AT3G54420	Chitinase class IV (ATEP3)	3.38	3E-010	2.38	3.36E-005	0.77	1.11E-002	3.07	6.90E-005
Lipid metabolism										
MDP0000193678	AT3G15850	Fatty acid desaturase 5 (FAD5)	2.17	9.02E-007	1.46	1.79E-003	1.16	3.33E-003	1.37	1.29E-003
MDP0000185343	AT5G22500	Fatty acid Reductase (FAR1)	1.14	2.21E-005	0.01	9.67E-001	0.63	3.30E-002	0.67	2.96E-002
MDP0000523183	AT3G12120	Fatty acid desaturase 2 (FAD2)	0.00	9.92E-001	1.15	1.44E-004	0.08	8.46E-001	0.34	1.97E-001
MDP0000190132	AT3G11170	Fatty acid desaturase 7 (FAD7)	1.00	1.53E-004	1.43	2.98E-005	-0.36	3.07E-001	-0.17	7.79E-001
Response to dehydration										
MDP0000273588	AT1G10370	Early response to dehydration 9 (ERD9)	0.88	2.25E-004	2.01	2.14E-006	-0.37	3.27E-001	-0.32	1.82E-001
MDP0000950619	AT4G39330	Mannitol dehydrogenase, putative	0.71	1.22E-003	1.04	2.99E-004	0.36	1.06E-001	-0.03	8.75E-001
MDP0000123910	AT5G51970	Sorbitol dehydrogenase, putative	0.78	5.40E-004	1.37	1.20E-004	-0.13	5.66E-001	0.19	3.96E-001
Lignin metabolism/accumulation										
MDP0000414002	AT2G23910	Cinnamoyl-CoA reductase-related (CRR)	1.03	2.87E-004	2.60	2.03E-007	-0.55	7.19E-002	-0.46	9.09E-002
MDP0000268879	AT5G19440	Cinnamyl-alcohol dehydrogenase (CAD)	0.92	1.29E-004	0.70	4.15E-003	0.49	4.91E-002	-0.06	8.59E-001
MDP0000293578	AT1G65060	4-coumarate:CoA ligase 3 (4CL3)	0.70	1.35E-003	1.90	1.38E-004	-0.13	5.69E-001	-0.02	9.72E-001
MDP0000139075	AT2G37040	Phenylalanine ammonia-lyase 1 (PAL1)	1.03	4.37E-005	1.65	1.52E-005	-0.57	2.63E-001	-0.17	6.51E-001
MDP0000876184	AT2G30490	Cinnamate-4-hydroxylase (C4H)	0.05	8.30E-001	1.53	4.81E-004	-0.12	5.68E-001	-0.37	3.91E-001
MDP0000242006	AT4G35350	Xylem cysteine peptidase (XCP1)	-0.01	9.50E-001	0.89	4.11E-003	1.16	4.31E-003	-0.47	1.17E-001
Sugar synthesis/transport										
MDP0000250070	AT3G43190	Sucrose synthase (SUS4)	-0.47	2.10E-002	-1.77	6.15E-006	0.19	6.29E-001	0.25	3.08E-001
MDP0000227381	AT1G78580	Trehalose-6-phosphate synthase (TPS1)	-0.22	2.36E-001	-1.60	1.22E-005	0.65	1.87E-001	0.26	3.22E-001
MDP0000262252	AT1G35910	Trehalose-6-phosphate phosphatase, putative	-1.13	3.51E-004	-2.74	7.39E-006	0.92	8.09E-002	0.43	1.24E-001
MDP0000818877	AT2G21250	Mannose 6-phosphate reductase, putative	-1.03	1.07E-003	-1.02	3.86E-004	0.49	1.83E-001	0.55	1.07E-001
MDP0000152142	AT1G11260	Sugar transporter 1 (STP1)	-0.78	9.41E-004	-1.12	1.67E-004	0.21	3.67E-001	-1.28	1.85E-002
MDP0000688348	AT3G18830	Polyol transporter 5 (PLT5)	-1.03	1.93E-004	-0.75	4.99E-003	0.14	6.99E-001	-0.53	4.73E-002
Transcription factors										
MDP0000400129	AT5G52020	AP2 domain-containing protein	-0.28	1.25E-001	-1.12	2.95E-003	0.56	3.90E-002	0.30	4.38E-001
MDP0000390121	AT5G07310	AP2 domain-containing transcription factor, putative	-0.39	7.98E-002	-1.16	1.39E-004	-0.19	4.53E-001	-0.16	4.72E-001
MDP0000861708	AT1G64380	AP2 domain-containing transcription factor, putative	-1.08	1.10E-004	-1.25	7.48E-005	0.27	4.93E-001	0.76	5.57E-002
MDP0000615948	AT2G46680	Arabidopsis thaliana homeobox 7 (ATHB-7)	-0.89	4.36E-004	-1.97	2.00E-006	0.64	4.58E-002	0.82	1.57E-002
MDP0000804929	AT1G75820	CLAVATA 1 (CLV1)	-1.04	1.13E-004	-0.28	2.01E-001	0.08	7.91E-001	-0.41	2.06E-001
MDP0000005879	AT4G32880	Arabidopsis thaliana homeobox 8 (ATHB-8)	0.1	5.75E-001	0.67	5.22E-003	-0.73	7.91E-002	-0.46	1.66E-001
MDP0000251484	AT1G52150	Arabidopsis thaliana homeobox 15 (ATHB-15)	0.44	2.34E-002	0.72	5.18E-003	-0.50	3.98E-002	-0.08	8.06E-001
MDP0000180683	AT3G04070	Arabidopsis NAC domain protein 47 (ANAC047)	-0.27	2.09E-001	-1.32	5.80E-005	0.53	1.42E-001	0.43	2.08E-001
MDP0000232050	AT5G61430	Arabidopsis NAC domain protein 100 (ANAC100)	0.00	9.86E-001	-1.39	1.02E-004	0.33	3.08E-001	0.65	2.94E-002
MDP0000240094	AT5G64530	Arabidopsis NAC domain protein 104 (ANAC104)	-0.25	2.69E-001	-2.87	1.73E-007	0.11	7.04E-001	-0.17	4.48E-001
MDP0000258530	AT1G01720	Arabidopsis NAC domain protein 2 (ATAF1)	-0.51	3.13E-002	-1.14	1.53E-004	0.64	8.69E-002	0.29	2.09E-001
MDP0000481448	AT1G69490	Nap-like transcription factor (NAP)	0.11	5.43E-001	-1.01	7.97E-004	0.66	1.02E-001	0.16	6.55E-001
MDP0000283092	AT1G33060	Arabidopsis NAC domain protein 014 (ANAC014)	-1.42	2.83E-005	-0.96	5.23E-004	0.13	6.90E-001	-0.26	3.58E-001
MDP0000320563	AT3G03200	Arabidopsis NAC domain protein 45 (ANAC045)	-1.19	4.74E-004	-0.83	2.47E-003	0.03	8.74E-001	-0.33	1.85E-001
MDP0000440829	AT3G10480	Arabidopsis NAC domain protein 50 (ANAC050)	-1.23	6.37E-005	-0.94	5.73E-004	0.15	5.13E-001	-0.57	3.82E-002
MDP0000278387	AT4G35580	No apical meristem (NAM) family protein	-1.26	1.11E-004	-0.84	1.43E-003	-0.10	6.94E-001	-0.18	5.23E-001
Phytohormone metabolism/signaling/response										
MDP0000138111	AT5G50760	Auxin-responsive family protein	0.04	8.50E-001	-1.57	2.18E-005	-0.17	4.97E-001	0.06	7.72E-001
MDP0000127291	AT4G34760	Auxin-responsive family protein	-0.19	3.61E-001	-1.23	1.24E-004	1.00	1.28E-002	0.28	2.66E-001
MDP0000810244	AT5G50760	Auxin-responsive family protein	-0.28	1.31E-001	-1.58	3.65E-005	-0.24	2.60E-001	-0.08	7.25E-001
MDP0000256199	AT3G63440	Cytokinin oxidase/dehydrogenase 6 (CKX6)	-1.28	1.19E-004	-2.41	1.48E-006	0.05	8.40E-001	0.21	5.45E-001
MDP0000279125	AT5G21482	Cytokinin oxidase 7 (CKX7)	-0.76	6.88E-004	-0.36	7.53E-002	0.38	1.94E-001	0.28	3.25E-001
MiR										
Md_miR166i	MiR166	MiR166	-0.56	6.46E-003	-0.72	6.43E-003	0.04	8.61E-001	-0.48	1.21E-001
Cell wall hydrolysis/modification										
MDP0000047586	AT2G44480	glycosyl hydrolase family 1 protein	1.30	6.13E-004	-0.03	8.67E-001	0.10	6.32E-001	-0.12	5.70E-001
MDP0000516992	AT5G05340	peroxidase, putative	2.56	2.88E-004	2.18	3.26E-003	0.17	4.25E-001	1.68	3.71E-003
MDP0000678562	AT4G33420	peroxidase, putative	-0.13	4.57E-001	1.13	2.39E-004	-0.16	4.47E-001	-0.11	6.07E-001
MDP0000545323	AT4G21960	Peroxidase 42 (PRXR1)	-0.16	4.46E-001	1.59	2.66E-005	-0.01	9.56E-001	-0.15	5.58E-001
MDP0000240772	AT5G03260	Laccase 11 (LAC11)	-0.51	1.17E-002	1.14	5.13E-004	0.03	9.06E-001	-0.29	2.36E-001
MDP0000127409	AT2G29130	Laccase 2 (LAC2)	0.65	2.54E-003	1.02	4.19E-004	-0.19	3.61E-001	0.71	1.13E-001
MDP0000816843	AT5G05390	Laccase 12 (LAC12)	1.54	2.86E-002	1.80	2.26E-002	0.69	1.22E-002	1.38	1.20E-003
MDP0000237964	AT5G60020	Laccase 17 (LAC17)	-0.62	4.06E-003	1.33	3.32E-004	-0.15	4.58E-001	-0.27	2.46E-001
MDP0000654233	AT3G09220	Laccase 7 (LAC7)	1.41	2.43E-002	1.69	3.89E-002	-0.21	3.13E-001	0.72	4.99E-002

difference between the central and lateral fruit AZ. This phase might correspond to a period during which the AZ cells acquire competence to react to abscission signals. Our differential gene expression analysis showed that no transcript was differentially expressed specifically during this phase. However, we identified several genes up-regulated in L1 pedicels during the three phases investigated. We found that genes involved in the stress response were largely induced in L1 pedicels, indicating an activation of protection systems during abscission. The expression of chitinase B1 (CHIB1) and allergen family proteins in the AZ had previously been reported in tomato (Nakano et al., 2013) and *Sambucus nigra* (Ruperti et al., 1999), respectively. Consistent with the observed fruit growth arrest, genes involved in sugar synthesis and transport were also down-regulated in L1 pedicels throughout the three phases investigated. The highly significant differential expression level of trehalose-6-phosphatase suggests a role for this gene in abscission induction. A role for this protein as a signal induced by nutritional stress had previously been suggested by Alferez et al. (2007) and Botton et al. (2011).

During the second phase, which corresponds to the activation of the abscission process, dividing cells were observed within the AZ of L1 pedicels. Cell division prior to abscission is not essential to the separation process in many species. For instance, cell division is absent in the pedicel of tobacco (*Nicotiana tabacum*; Jensen and Valdovinos, 1967), tomato (Roberts et al., 1984), *Citrus* spp. (Wilson and Hendershott, 1968), and Arabidopsis (Patterson, 2001). This cell division step was observed in soybean (*Glycine max*; Webster, 1968) and *Salix* and *Castanea* spp. (van Doorn and Stead, 1997). However, in *Salix* spp., cell division occurred in a layer beneath the actual separation layer, while in *Castanea* spp., cell division was observed after abscission. Despite the observation of dividing cells in the region of the AZ in L1 pedicels, we did not identify differentially expressed genes associated with cell division. Change in the expression of these particular genes may have been attenuated due to the method used for sampling and to the rather small proportion of dividing cells in the tissues analyzed.

In all the species in which cell division was observed, the newly formed cells became involved in the formation of protecting tissue containing suber or lignin. In our apple L1 pedicels, during the third phase of abscission, we also observed that the walls of cells located on the pedicel side became heavily impregnated with lignin, while cells located on the bourse side accumulated suberin depositions. It has been proposed that plants activate these defense responses as a protective measure before shedding (Roberts et al., 2002). This idea is consistent with our histological observations and supported by transcript expression analysis. Indeed, we observed that genes involved in suberin biosynthesis were overexpressed in L1 pedicels. Suberin is a polymer of fatty acid derivatives linked by ester bonds. It is mostly deposited on the inner face of primary cell walls and has a role in resistance to pathogens and in preventing water loss following organ abscission (Beisson et al., 2012). In our analysis, we found that key genes involved in the suberin biosynthesis pathway were overexpressed in L1 pedicels during the last stage of the abscission process (Fig. 9), including glycerol-3-phosphate acyltransferases, aliphatic suberin feruloyl transferase, hydroxylase of root suberized tissue, root aliphatic plant hydroxylase1, Fatty acyl-CoA reductase1, and ABC transporter G11. Major genes associated with lignin biosynthesis were also strongly up-regulated in L1 AZs during the last stage of abscission (Fig. 9), including Arabidopsis cinnamate 4-hydroxylase, OPC-8:CoA ligase1, Cinnamoyl CoA Reductase1, cinnamyl alcohol dehydrogenase, and ferulate 5-hydroxylase. Up-regulation of these genes is consistent with our observation of lignin accumulation in the walls of cells located on the pedicel side.

Further analysis using scanning electron microscopy indicated extensive cell wall and middle lamella degradation in the separation layer. At that stage, the apple fruitlet AZ differentiated as a plate of 10 to 15 isodiametrically flattened cells and traversed the cortex, pith, and vascular bundles, although the AZ appeared disorganized through the vascular tissues. Consistent with these observations, we identified differentially expressed genes associated with cell wall degradation in the last stage of the abscission process. Most of the hydrolases overexpressed in the last phase of L1 pedicel abscission are known to act on glycosyl bonds and include endotransglycosylase-related proteins, β-galactosidases, pectinesterases (Fig. 9), laccases, and various glycosyl hydrolases. To further break down the glycosidic bonds of pectins composing the middle lamella, several polygalacturonases were also found overexpressed in L1 AZs. These include homologs of AT2G43890, AT3G07970 (Fig. 9), and AT3G59850, which were previously found overexpressed in Arabidopsis and tomato pedicel AZs (Kim and Patterson, 2006; González-Carranza et al., 2007; Nakano et al., 2013). In parallel with the expression of cell wall-modifying enzymes, we also identified several genes associated with senescence, response to dehydration, and desiccation (Table III), which is consistent with pedicel drop.

Finally, our transcriptomic data suggest a central role for hormone-related genes throughout the three phases described previously. The current model accepted for abscission implies that auxin, produced by the subtending fruitlet, is translocated down the pedicel through the AZ, delaying its activation by reducing the sensitivity of the AZ to ethylene (van Doorn and Stead, 1997). Our transcriptomic analysis showed that 1-aminocyclopropane-1-carboxylic acid oxidase, involved in ethylene biosynthesis, was up-regulated in L1 AZ. In parallel, we found that genes homologous to ETHYLENE RESPONSE FACTOR1 (ERF1) and ERF2 (Fig. 9) were up-regulated during the three time points investigated, together with a down-regulation of a MAJOR LATEX PROTEIN-related protein. A previous study showed that ethylene played a role in the

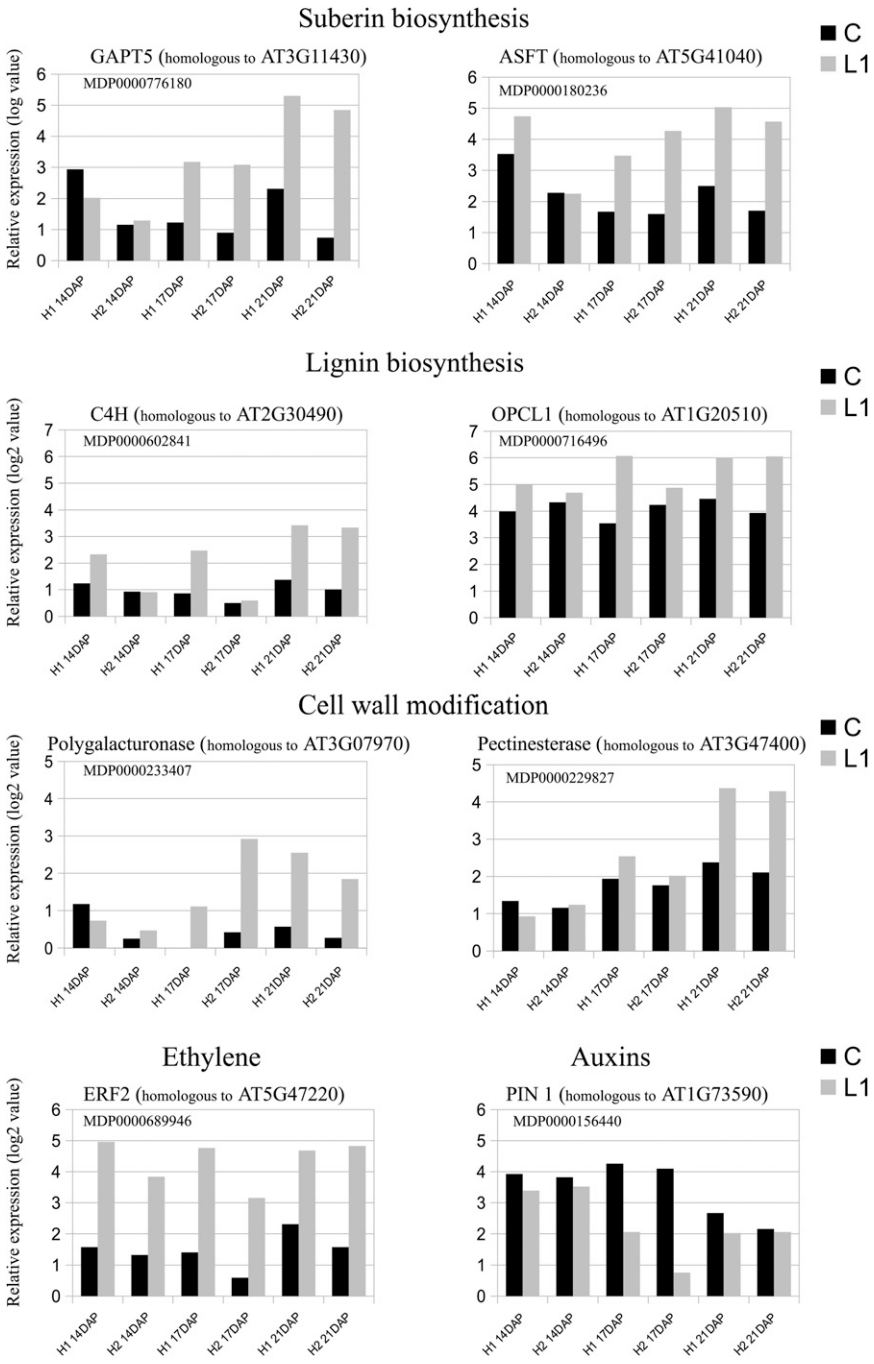

Figure 9. Kinetics of the expression values of genes differentially expressed between central (C) and L1 AZs of the two X3177 apple biological replicates (H1 and H2) as determined by microarray analysis at three developmental stages (14, 17, and 21 DAP). The kinetics of expression values of selected genes involved in suberin biosynthesis, lignin biosynthesis, cell wall modification, ethylene response factor, and auxin transport are represented. The transcript levels were normalized with the lowess method. Intensity values were then subtracted from the background.

negative regulation of MAJOR LATEX PROTEIN in peach (*Prunus persica*) AZ and that this gene plays a preemptive role in abscission-related plant defense (Ruperti et al., 2002). These genes can thus be used as markers of ethylene overexpression in L1 pedicels. In the mean time, we identified a down-regulation of auxin response factors and the PIN1 transporter gene (Fig. 9) at 17 DAP. This differential expression of genes is in accordance with the accepted model for abscission and confirms that these hormones play a major role to stimulate AZ development in apple. Concurrently, jasmonic acid carboxyl methyltransferases were overexpressed in L1 AZ. Jasmonic acid carboxyl methyltransferases are known to respond to auxin and ethylene stimulus and were shown to be overexpressed in response to wounding in Arabidopsis (Seo et al., 2001). Meanwhile, we observed an increased expression of GA 2-oxidases from the early stages of abscission as well as cytokinin oxidases in the last stage of the process, which is consistent with previous studies (Eccher et al., 2013) and indicates a decrease of active GA and cytokinin levels in the L1 pedicel.

Table III. *Selection of differentially expressed genes in apple pedicel AZs*

The gene identifier is reported along with the Arabidopsis gene homolog, a short annotation, and the pattern of expression in both biological replicates at stages 14, 17, and 21 DAP. The complete list and further details, are available in Supplemental Table S3.

Apple Gene Identification	Arabidopsis Homolog	Annotation	H1 14DAP		H2 14DAP		H1 17DAP		H2 17DAP		H1 21DAP		H2 21DAP	
			log² rat	P	log² rat	P	log² rat	P	log² rat	P	log² rat	P	log² rat	P
Defense response														
MDP0000310481	AT5G24090	acidic endochitinase (CHIB1)	2.47	1.59E-004	1.19	7.75E-003	3.45	1.81E-005	1.51	1.52E-002	1.77	2.12E-003	2.89	1.98E-004
MDP0000119517	AT1G24020	Bet v I allergen family protein	3.31	3.76E-004	2.52	1.03E-004	4.5	6.68E-006	1.52	5.99E-004	3.61	1.64E-005	4.4	1.72E-004
MDP0000277802	AT1G14930	major latex protein-related (MLP)	-0.38	1.84E-001	-0.7	2.53E-002	-1	3.93E-003	-0.63	2.96E-002	-2.17	2.00E-004	-1.74	1.33E-003
MDP0000782085	AT3G04720	PATHOGENESIS-RELATED (PR4)	4.01	2.39E-004	0.21	6.11E-001	4.05	8.47E-006	2.92	3.72E-004	2.64	1.70E-004	4.26	7.93E-005
Transcription factors														
MDP0000121265	AT5G61430	Arabidopsis NAC domain containing protein 100 (ANAC100)	3.73	2.76E-005	2.45	4.73E-005	4	3.38E-006	1.64	2.18E-003	3.56	4.85E-006	4.67	7.63E-006
MDP0000140229	AT2G46770	NAC secondary wall thickening promoting factor (NST1)	-1.72	6.86E-003	0.22	6.03E-001	0.26	5.16E-001	0.86	8.32E-002	-2.28	2.67E-004	-3.1	5.30E-005
Phytohormone metabolism/signaling/response														
MDP0000235313	AT3G23240	ETHYLENE RESPONSE FACTOR 1 (ERF1)	2.9	7.15E-004	2.87	3.30E-005	1.49	7.06E-004	0.71	2.69E-002	1.98	3.61E-004	2.47	2.02E-004
MDP0000689946	AT5G47220	ETHYLENE RESPONSE FACTOR 2 (ERF2)	3.44	1.24E-004	2.53	1.89E-004	3.36	2.56E-005	2.54	5.27E-005	2.38	2.61E-004	3.28	3.31E-005
MDP0000250254	AT1G62960	ACC SYNTHASE 10 (ACS10)	1.86	5.36E-004	0.48	7.89E-002	2.36	5.43E-005	0.37	1.39E-001	2.1	7.32E-005	1.83	4.41E-004
MDP0000200896	AT2G19590	ACC OXIDASE 1 (ACO1)	1.33	9.94E-003	0.2	4.36E-001	2.41	6.07E-005	0.1	6.89E-001	2.97	4.09E-005	3.73	9.96E-006
MDP0000137705	AT1G78440	GIBBERELLIN 2-OXIDASE 1 (GA2OX1)	3.82	4.36E-005	2.4	3.74E-005	2.19	7.22E-005	-0.55	4.89E-002	3.38	4.52E-006	3.14	5.51E-005
MDP0000735747	AT1G02400	GIBBERELLIN 2-OXIDASE 6 (GA2OX6)	3.59	1.62E-004	1.7	5.67E-003	2.78	3.13E-004	0.75	1.34E-001	2.3	7.05E-004	2.91	7.77E-004
MDP0000132878	AT4G21200	GIBBERELLIN 2-OXIDASE 8 (GA2OX8)	2.62	6.69E-004	2.21	1.96E-004	1.52	2.00E-003	1.57	5.32E-004	1.9	2.61E-004	2.63	3.59E-004
MDP0000929655	AT1G59750	AUXIN RESPONSE FACTOR 1 (ARF1)	0.1	6.79E-001	0.55	5.62E-002	-1.15	1.95E-003	-2.19	9.93E-005	-0.63	4.28E-002	-0.03	9.13E-001
MDP0000912733	AT4G30080	AUXIN RESPONSE FACTOR 16 (ARF16)	-0.12	5.91E-001	0.28	2.55E-001	-1.52	5.30E-004	-2.83	2.34E-005	-0.61	4.42E-002	0.42	1.56E-001
MDP0000931116	AT5G62000	AUXIN RESPONSE FACTOR 2 (ARF2)	-0.14	6.36E-001	-0.38	2.35E-001	-3.13	6.72E-005	-4.37	8.09E-006	-1.18	5.92E-003	-0.38	2.70E-001
MDP0000412781	AT5G60450	AUXIN RESPONSE FACTOR 4 (ARF4)	-0.73	2.23E-002	-0.3	2.28E-001	-1.4	8.55E-004	-2.94	2.41E-005	-1.24	1.67E-003	0.36	2.65E-001
MDP0000294251	AT5G37020	AUXIN RESPONSE FACTOR 8 (ARF8)	-0.46	1.09E-001	-0.27	2.77E-001	-1.75	7.61E-004	-3.52	1.52E-005	-0.99	3.53E-002	-0.32	4.86E-001
MDP0000156440	AT1G73590	PIN-FORMED 1 (PIN1)	-0.49	2.57E-001	-0.29	4.06E-001	-2.2	2.34E-004	-3.38	6.55E-005	-0.64	9.64E-002	-0.08	8.53E-001
MDP0000813805	AT3G14440	NINE-CIS-EPOXYCAROTENOID DIOXYGENASE3 (NCED3)	2.92	2.40E-004	2.24	4.88E-004	2.35	1.94E-004	0.66	5.12E-002	1.8	2.41E-004	2.65	6.81E-005
MDP0000246006	AT1G78390	NINE-CIS-EPOXYCAROTENOID DIOXYGENASE 9 (NCED9)	1.49	2.25E-002	0.27	6.55E-001	1.4	7.51E-004	0.03	9.18E-001	2.23	1.00E-004	2.04	9.23E-004
MDP0000386460	AT1G30100	NINE-CIS-EPOXYCAROTENOID DIOXYGENASE 5 (NCED5)	1.99	1.86E-003	0	9.96E-001	1.98	2.87E-004	-0.59	7.17E-002	2.07	7.96E-005	2.87	3.80E-005
MDP0000165684	AT3G43600	ALDEHYDE OXIDASE 2 (AAO2)	1.68	1.83E-003	0.27	3.24E-001	2.1	3.12E-004	0.4	1.51E-001	1.76	5.45E-004	1.94	1.01E-003
MDP0000437033	AT4G26080	ABA INSENSITIVE 1 (AB11)	2.17	3.35E-004	1.1	2.76E-003	2.79	3.32E-005	0.51	6.71E-002	2.25	5.38E-005	2.31	1.43E-004
MDP0000893203	AT5G57050	ABA INSENSITIVE 2 (ABI2)	1.65	1.10E-003	0.21	3.94E-001	2.24	6.84E-005	0.57	4.55E-002	2.23	5.75E-005	1.88	3.91E-004
MDP0000186091	AT1G19640	JASMONIC ACID CARBOXYL METHYLTRANSFERASE (JMT)	1.13	9.07E-003	0.61	1.14E-001	1.92	2.33E-004	0.3	2.39E-001	1.92	2.18E-004	2.95	4.99E-005
MDP0000279125	AT5G21482	CYTOKININ OXIDASE 7 (CKX7)	0.96	1.06E-002	0.26	2.93E-001	1.64	3.56E-004	0.32	2.11E-001	1.57	7.49E-004	1.9	6.32E-004
MDP0000234983	AT1G75450	CYTOKININ OXIDASE 5 (CKX5)	0.95	1.08E-002	0.08	7.23E-001	1.4	8.30E-004	0.55	5.53E-002	1.19	4.24E-003	2.18	2.24E-004
MDP0000293966	AT3G63440	CYTOKININ OXIDASE 6 (CKX6)	1.64	2.29E-003	1.03	3.57E-003	1.21	3.22E-003	0.24	3.23E-001	1.69	4.25E-004	2.02	3.60E-004
Sugar synthesis/transport														
MDP0000824990	AT5G49190	SUCROSE SYNTHASE 2 (SUS2)	-1.05	6.65E-003	-0.61	4.19E-002	-1.57	4.12E-004	-1.15	2.53E-003	-0.4	1.68E-001	-1.07	7.38E-003
MDP0000462673	AT4G02280	SUCROSE SYNTHASE 3 (SUS3)	-0.27	3.30E-001	-0.25	3.04E-001	-1.37	1.03E-003	-2.47	4.79E-005	-0.84	1.20E-002	-0.46	1.25E-001
MDP0000214583	AT1G09960	SUCROSE TRANSPORTER 4 (SUT4)	-0.6	1.84E-001	-0.47	1.53E-001	-1.6	7.12E-004	-2.71	5.28E-005	-1.01	1.37E-002	-0.36	2.59E-001
MDP0000798684	AT1G60470	GALACTINOL SYNTHASE 4 (GOLS4)	-1.47	1.76E-003	0.19	4.42E-001	-0.12	6.01E-001	0.9	8.90E-003	-1.84	1.66E-004	-2.84	4.04E-005
MDP0000311007	AT1G35910	trehalose-6-phosphate phosphatase. putative	2.65	5.00E-004	2.14	1.27E-004	2.15	1.76E-004	0.87	1.93E-002	1.82	4.76E-004	2.75	5.19E-005
MDP0000848217	AT1G78090	TREHALOSE-6-PHOSPHATE PHOSPHATASE (TPPB)	0.15	6.15E-001	-0.12	6.33E-001	0.06	8.09E-001	-0.19	4.90E-001	3.19	1.44E-005	2.79	1.76E-004
Cell wall hydrolysis/modification														
MDP0000278332	AT2G25630	glycosyl hydrolase family 1 protein	0.18	6.58E-001	-0.05	8.58E-001	1.69	1.60E-003	1.27	4.30E-003	2.28	2.45E-004	3.18	1.25E-004
MDP0000163547	AT4G16260	glycosyl hydrolase family 17 protein	3.89	5.79E-004	-0.06	8.08E-001	4.11	1.98E-005	2.67	4.30E-005	3.02	2.87E-005	4.25	1.71E-005
MDP0000513880	AT4G19810	glycosyl hydrolase family 18 protein	4.43	7.16E-005	0.35	2.68E-001	4.02	3.56E-005	3.79	8.95E-005	2.3	3.01E-004	4.27	2.76E-005
MDP0000516623	AT3G59850	polygalacturonase. putative / pectinase. putative	4.44	4.43E-005	-0.42	1.09E-001	5.35	9.94E-006	1.83	2.95E-004	3.48	6.30E-006	4.78	2.07E-006
MDP0000845685	AT2G43890	polygalacturonase. putative / pectinase. putative	1.69	6.76E-003	0.09	7.06E-001	2.25	1.58E-004	-0.05	8.14E-001	3.91	3.83E-005	4.87	5.76E-005
MDP0000233407	AT3G07970	polygalacturonase. putative / pectinase. putative	-0.4	1.32E-001	0.23	3.45E-001	1.17	2.29E-003	2.47	2.08E-004	1.99	1.27E-004	1.6	8.58E-004
MDP0000139079	AT3G09220	Laccase 7 (LAC7)	3.14	1.65E-004	-0.76	2.00E-002	2.47	6.68E-004	2.45	1.87E-004	2.73	3.69E-004	2.43	2.77E-003
MDP0000228494	AT2G40610	EXPANSIN A8 (EXPA8)	-3.45	1.79E-004	-0.38	4.54E-001	-0.39	2.35E-001	0.19	5.31E-001	-2.77	1.26E-005	-2.34	1.14E-004
MDP0000139485	AT1G32170	XYLOGLUCAN ENDOTRANSGLYCOSYLASE 4 (XTR4)	2.9	9.58E-005	1.23	2.28E-003	3.34	6.99E-006	1.25	4.59E-003	3.02	7.04E-006	3.12	4.78E-005
MDP0000320017	AT4G25810	XYLOGLUCAN ENDOTRANSGLYCOSYLASE 6 (XTR6)	2.11	5.18E-004	0.32	1.98E-001	2.47	3.82E-005	0.93	1.09E-002	1.73	3.29E-004	2.18	3.99E-004
MDP0000263744	AT4G14130	XYLOGLUCAN ENDOTRANSGLYCOSYLASE 7 (XTR7)	1.11	1.14E-002	0.47	1.11E-001	0.65	2.80E-002	-0.82	1.05E-002	1.65	4.25E-004	3.08	2.68E-005
MDP0000198727	AT4G25820	XYLOGLUCAN ENDOTRANSGLYCOSYLASE 9 (XTR9)	0.17	5.37E-001	0.37	1.78E-001	0.09	7.10E-001	-0.07	7.71E-001	1.02	6.68E-003	2.05	8.49E-004
MDP0000127542	AT3G52840	Beta-galactosidase putative	3.01	7.37E-004	1.86	8.73E-004	3.17	6.23E-005	1.5	4.21E-003	2.39	4.57E-004	2.13	1.35E-003
MDP0000174791	AT5G09760	pectinesterase family protein	2.02	5.37E-004	0.77	1.85E-002	2.2	7.48E-005	2.02	1.63E-004	1.59	4.08E-004	2.41	9.74E-005
MDP0000639167	AT2G45220	pectinesterase family protein	4.19	6.04E-004	0.06	8.33E-001	3.12	1.58E-003	0.69	1.20E-001	2.31	8.83E-005	4.39	1.02E-005
MDP0000229827	AT3G47400	pectinesterase family protein	-0.35	1.70E-001	0.09	7.04E-001	0.6	3.19E-002	0.23	3.32E-001	1.99	1.58E-004	2.2	1.69E-004
MDP0000154985	AT4G33220	pectinesterase family protein	0.21	4.41E-001	0.01	9.54E-001	0.64	2.60E-002	0.01	9.49E-001	1.68	3.56E-004	2	4.91E-004
MDP0000194940	AT1G16120	WALL ASSOCIATED KINASE-LIKE 1 (WAKL1)	3.47	1.15E-004	1.41	1.17E-003	2.33	2.61E-004	1.07	3.24E-003	2.53	5.32E-005	2.69	1.50E-004
MDP0000681106	AT1G16130	WALL ASSOCIATED KINASE-LIKE 2 (WAKL2)	2.37	4.93E-004	0.89	1.18E-002	2.33	1.35E-004	0.38	1.57E-001	2.62	4.22E-005	2.67	1.13E-004
MDP0000426154	AT1G16150	WALL ASSOCIATED KINASE-LIKE 4 (WAKL4)	3.75	1.24E-004	1.73	7.98E-004	2.27	9.04E-005	1.22	3.79E-003	2.67	6.41E-005	2.39	3.54E-004
Dehydration/Ripening responsive/Senescence														
MDP0000321774	AT5G51070	EARLY RESPONSIVE TO DEHYDRATION 1 (ERD1)	1.84	6.45E-004	0.15	5.27E-001	2.84	2.84E-005	0.64	3.06E-002	2.72	3.18E-005	2.85	8.37E-005
MDP0000213383	AT5G65380	ripening-responsive protein. putative	0.99	9.35E-003	0.05	8.42E-001	2.86	3.00E-005	1.56	7.22E-004	2.32	3.86E-005	3.14	3.47E-005
MDP0000113336	AT1G17020	SENESCENCE-RELATED GENE 1 (SRG1)	2.95	1.35E-004	0.33	2.10E-001	3.51	8.89E-006	1.87	3.64E-004	2.37	8.12E-005	2.88	6.19E-005
MDP0000238720	AT5G45890	SENESCENCE-ASSOCIATED GENE 12 (SAG12)	1.57	1.26E-003	-0.02	9.33E-001	1.25	1.64E-003	0.35	1.72E-001	1.24	1.76E-003	1.72	5.99E-004
MDP0000385497	AT4G02380	SENESCENCE-ASSOCIATED GENE 21 (SAG21)	1.33	2.39E-003	0.98	4.82E-003	1.81	3.20E-004	0.38	1.29E-001	1.87	1.63E-004	1.97	3.28E-004
Receptor-like protein kinase														
MDP0000396340	AT5G65710	HAESA-LIKE 2 (HSL2)	1.45	2.26E-003	0.53	5.92E-002	1.42	7.54E-004	0.91	7.16E-003	1.33	1.10E-003	2.03	2.60E-004
MDP0000588798	AT1G51660	MITOGEN-ACTIVATED PROTEIN KINASE KINASE 4 (MKK4)	2.12	1.83E-003	0.63	5.03E-002	2.3	2.66E-004	1.04	5.58E-003	1.9	1.14E-003	2.06	1.13E-003
MDP0000237742	AT3G45640	MITOGEN-ACTIVATED PROTEIN KINASE 3 (MPK3)	2.09	1.67E-003	0.7	4.26E-002	1.81	3.13E-004	0.58	6.29E-002	1.62	1.33E-003	1.72	1.04E-003
Cellulose biosynthesis														
MDP0000470441	AT5G17420	IRREGULAR XYLEM 3 (IRX3)	-2.38	3.77E-004	0.72	3.75E-002	0.37	1.94E-001	0.98	1.02E-002	-2.78	1.24E-005	-3.02	3.11E-005
MDP0000126039	AT2G37090	IRREGULAR XYLEM 9 (IRX9)	-3.16	5.27E-004	0.73	8.09E-002	0.04	9.13E-001	0.3	3.63E-001	-3.38	3.77E-005	-3.13	1.37E-004
MDP0000883782	AT5G15630	COBRA-LIKE4 (COBL4)	-2.73	1.07E-004	0.9	6.62E-003	0.5	5.99E-002	0.85	1.10E-002	-2.81	1.13E-005	-2.4	1.04E-004
MDP0000320351	AT5G44030	CELLULOSE SYNTHASE 4 (CESA4)	-2.97	7.47E-005	0.83	9.48E-003	0.53	5.29E-002	0.94	6.35E-003	-3.25	4.75E-006	-2.93	3.27E-005
MDP0000214413	AT4G18780	CELLULOSE SYNTHASE 8 (CESA8)	-2.61	1.34E-004	0.53	7.35E-002	-0.15	6.60E-001	-0.08	7.94E-001	-3.24	9.73E-006	-2.71	2.40E-004
Suberin metabolism														
MDP0000776180	AT3G11430	GLYCEROL-3-PHOSPHATE ACYLTRANSFERASE 5 (GPAT5)	-0.87	1.72E-002	0.15	5.49E-001	1.95	1.43E-004	2.15	1.69E-004	3	9.84E-006	4.13	7.24E-006
MDP0000879217	AT5G58860	HORST / CYP86A1	-1.42	2.25E-003	0.24	3.60E-001	0.62	3.27E-002	2.92	3.40E-005	2.35	3.54E-005	1.57	4.87E-003
MDP0000234292	AT5G23190	RALPH / CYP86B1	-0.92	1.01E-002	0.11	6.57E-001	0.73	1.66E-002	2.22	8.66E-005	1.51	5.76E-004	1.05	7.44E-003
MDP0000185343	AT5G22500	FAR1 / acyl CoA reductase. putative	-1.86	4.85E-003	0.15	6.66E-001	1.17	1.69E-002	3.09	9.16E-005	2.31	4.54E-004	2.24	1.04E-003
MDP0000180236	AT5G41040	ASFT	1.27	5.42E-003	-0.02	9.28E-001	1.8	1.11E-003	2.64	2.54E-004	2.54	6.24E-005	2.89	3.36E-004
MDP0000150931	AT1G17840	ABCG11	0.48	1.29E-001	0.86	7.97E-003	1.62	4.57E-004	0.4	1.48E-001	1.06	4.34E-003	1.06	7.41E-003
Lignin metabolism														
MDP0000602841	AT2G30490	CINNAMATE-4-HYDROXYLASE (C4H)	1.14	1.01E-002	-0.01	9.78E-001	1.61	3.69E-004	0.06	8.06E-001	2.05	9.69E-005	2.34	1.61E-004
MDP0000716496	AT1G20510	OPC-8:0 COA LIGASE1 (OPCL1)	1.05	5.91E-003	0.37	1.47E-001	2.54	3.18E-005	0.62	4.27E-002	1.56	4.47E-004	2.14	2.02E-004
MDP0000268045	AT1G15950	CINNAMOYL COA REDUCTASE 1 (CCR1)	1.76	7.49E-004	0.32	2.05E-001	1.78	2.10E-004	0.61	3.30E-002	1.31	1.23E-003	1.46	1.55E-003
MDP0000290205	AT5G04330	ferulate-5-hydroxylase putative	1.15	2.25E-002	0.57	2.65E-001	2.38	1.11E-003	0.1	7.10E-001	2.21	3.95E-004	1.77	6.68E-004
MDP0000160603	AT5G19440	cinnamyl-alcohol dehydrogenase putative (CAD)	2.22	6.38E-004	0.66	5.05E-002	2.51	1.44E-004	0.73	1.67E-002	1.9	3.29E-004	2.04	8.53E-004

CONCLUSION

In apple, the thinning of young fruits during the early phases of development is a prerequisite to allow the plant to bring to maturity fruits of optimum commercial size and quality. In this study, we characterized the self-thinning capacity of the apple hybrid X3177, from the tree scale to the molecular scale, and over a period covering the main stages of flower and young fruit development.

On the basis of our results, we extended the model developed by Botton et al. (2011) and Eccher et al. (2013) to explain the naturally exacerbated dominance of central fruitlets over lateral ones (Fig. 10). Our work reveals that the majority of the corymbs of this hybrid bring to maturity only the central fruit while shedding all the lateral ones. We show that the central fruit pedicels develop a rare phenotype in the form of additional amphivasal vascular bundles located in the pith. To the best of our knowledge, this study provides one of the first examples of the identification of amphivasal bundles in dicots. These additional bundles develop before the onset of flowering and provide the central flower/fruit with additional resources such as sorbitol, allowing it to develop a strong dominance over the lateral ones. Global gene expression data indicate a general trend toward an up-regulation of genes involved in vascular tissue differentiation in central pedicels together with a down-regulation of genes involved in sugar transport in L1 pedicels, which is consistent with our hypothesis. Furthermore, we identified a strong up-regulation of genes involved in the stress response in L1 pedicels before the onset of abscission. However, a more targeted approach is necessary to identify the key genes triggering the localized development of these amphivasal bundles and to determine the heritability of this phenotype.

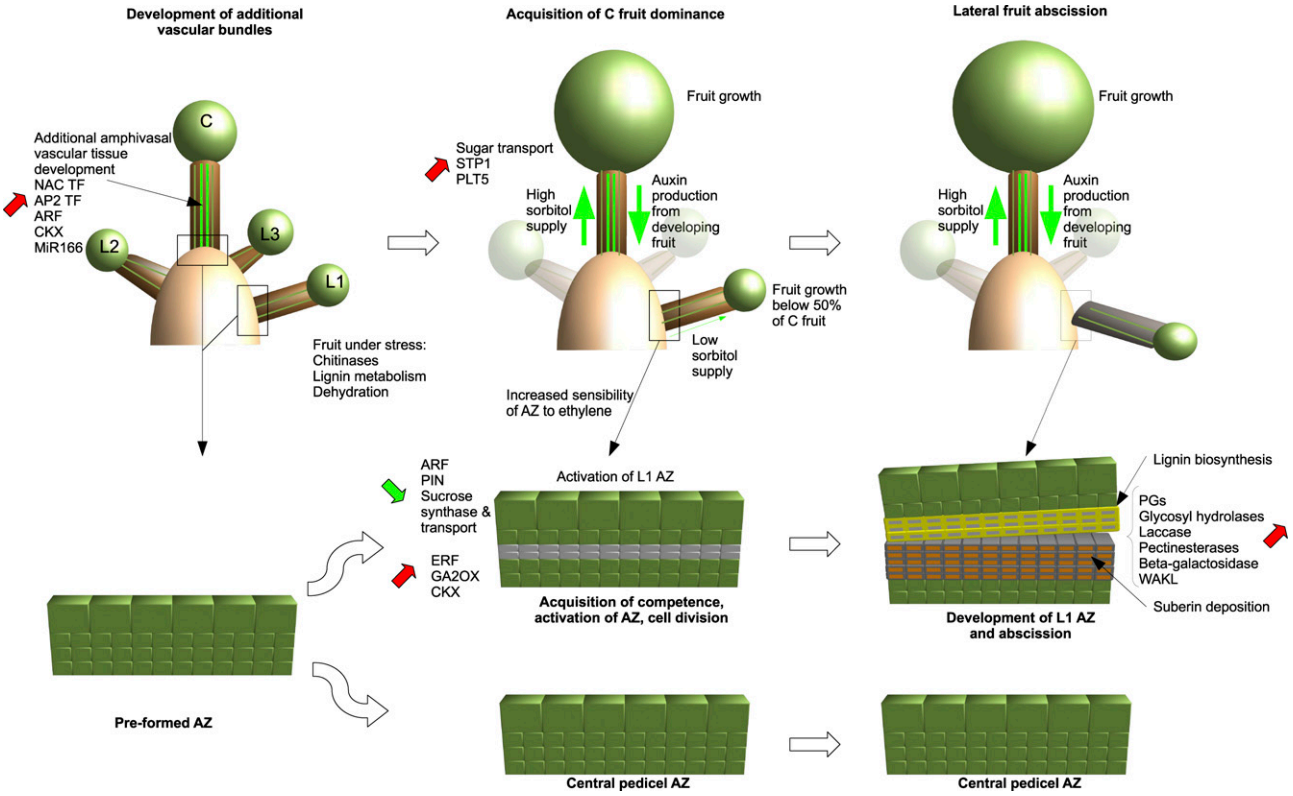

Figure 10. Model of the development of apple fruitlets and their respective AZs. This model was developed from the analyses of X3177 corymbs, pedicel vascular tissue, and AZ development. Data presented from analyses in this article are schematically summarized in relation to the relative positions of the fruitlets within the corymb. In this model, additional bundles develop early in the central fruit pedicel and may provide it with additional resources such as sorbitol, allowing it to develop a strong dominance over the lateral ones. Global gene expression data indicate a general trend toward an up-regulation of genes involved in vascular tissue differentiation in central pedicels together with a down-regulation of genes involved in sugar transport in L1 pedicels. AZ activation is triggered 4 to 5 d following lateral fruit growth arrest and is initiated with a cycle of cell divisions. Following the formation of layers of isodiametrically flattened cells, we observe a degradation of cell walls and middle lamella at the separation zone by multiple cell wall-modifying enzymes. Cells located on the pedicel side become impregnated with lignin, while cells located on the bourse side accumulate suberin depositions. C, Central fruitlet; L1, small lateral fruitlet; L2, medium lateral fruitlet; L3, big lateral fruitlet.

To further investigate the processes involved in the abscission of lateral fruitlets, we studied the kinetics of AZ development. We found that AZ activation was triggered 4 to 5 d following lateral fruit growth arrest and was initiated with a cycle of cell divisions. Following the formation of layers of isodiametrically flattened cells, we observed a degradation of cell walls and middle lamella at the separation zone. In parallel with this degradation, we observed that cells located on the pedicel side became heavily impregnated with lignin while cells located on the bourse side accumulated suberin depositions. Differential gene expression analysis of AZ formation compared with their immediate nonseparating neighbor matched our histological observations, and our results are in accordance with the accepted model for abscission. Our data confirm the major role of ethylene and auxin as well as cell wall-remodeling enzymes.

A better understanding of the mechanisms involved in the development of the self-thinning characteristic might allow in the future the introduction of this phenotype into elite apple breeding lines and will help control biennial bearing while reducing the application of fruit thinning chemicals.

MATERIALS AND METHODS

Plant Material

Experiments were carried out in 2011, 2012, and 2013 on X3177 apple (*Malus* × *domestica*) trees planted in 2005 and grafted onto cv M.9 rootstocks and on cv Ariane trees planted in 2004 and grafted onto cv Pajam2 rootstocks. X3177 is derived from a cross between cv Idared and cv Prima performed at the Institut National de la Recherche Agronomique station in Bordeaux in 1975. Trees were trained with standard horticultural practices at the Experimental Unit of the Institut National de la Recherche, with the exception of thinning treatments. Two trees of each genotype were used to obtain biological replicates. For both genotypes, each year, 50 to 60 corymbs per tree were selected on 1-year-old spurs at similar phenological stages. Flowers of each corymb were manually pollinated with a mixture of pollen at F1 stage (central flower open) to ensure that physiological drop was not caused by the lack of flower fertilization. All subsequent measures and sample harvest were performed using these hand-pollinated corymbs. All fruits were classified according to their abscission potential as described by Botton et al. (2011).

In 2011, central and L1 fruitlet diameters of cv Ariane and X3177 were monitored using 10 corymbs of each tree to identify differences in growth dynamics between fruits from F1 stage to 21 DAP. From the F1 stage to 21 DAP, 10 pedicels (without AZ) were harvested at each time point and stored appropriately for histological and gene expression studies. These samples were composed of a 1-cm section of pedicel located 5 mm above the AZ to about 5 mm below the flower/fruit base.

In 2012, pedicel development was investigated on both X3177 trees, from stage D3 (floral bud appearance, 10 d before pollination) to 22 DAP. Again, 10 pedicels (without AZ) per time point were regularly harvested from selected corymbs and stored for histological and gene expression studies. These samples were also composed of a 1-cm section of pedicel located 5 mm above the AZ to about 5 mm below the flower/fruit base.

In 2013, for both X3177 trees, fruitlet drop dynamics was monitored from 2 to 64 DAP. This was performed at the whole-tree scale by counting the fruits dropped onto nets previously spread underneath the trees. In addition, fruit drop was monitored on 30 selected corymbs (15 corymbs from each tree). These corymbs were selected on 1-year-old spurs located in the middle section of each tree at a similar phenological stage. Flowers of each corymb were manually pollinated with a mixture of pollen at F1 stage. Five AZs were collected on each X3177 tree at 14, 17, and 21 DAP and stored for histological and gene expression studies. These samples were composed of the AZ section together with 1 to 2 mm of neighboring tissues.

Additional experiments were conducted on hybrids descended from X3177. These included individuals derived from the crosses X3263 × X3259, cv Generos × X6681, and X7940 × X6681. Both X3263 and X6681 derive from a cross with X3177. Eighteen individuals derived from these crosses were selected based upon their mean number of fruits per corymb at maturity and classified as one fruit per corymb or several fruits per corymb. Pedicels from mature fruits derived from these selected individuals were collected in 2011, hand cut with a razor blade, and stained with toluidine blue before observation.

Histological Staining and Microscopy

Three methodologies were used to study vascular system and AZ development. The aim of the first experiment was to identify and characterize the different stages occurring during vascular bundle and AZ formation. For this, additional pedicels harvested from stage E2 to 21 DAP were hand cut with a razor blade, immersed in 70% (v/v) ethanol for 5 min, stained using 0.02% (w/v) acridine orange (Sigma), and rinsed twice in ultrapure water. Acridine orange is a nonspecific stain that has been mainly used to stain DNA, but plant cell walls also emit metachromatic fluorescence after staining with this compound. The green coloration is attributed to cellulose, while the red is attributed to lignins. When both compounds are present in important quantities, cell walls appear in yellow color (Abot, 2010). Images were acquired with a Nikon A1 confocal laser scanning microscope equipped with argon ion (488 nm) using a 10× air-immersion lens with a numerical aperture of 0.3. Under these conditions, the optical section thickness was approximately 7.5 mm and the z-scanning step was set accordingly at 7.5 mm. The excitation wavelength was 488 nm and the light emitted over 515 nm was collected using a long-pass filter.

The second experiment was aimed at finely characterizing the anatomical organization of vascular bundles and the AZ. For this, samples were fixed in 4% (v/v) glutaraldehyde in phosphate buffer (0.1 M, pH 7.2) for 3 h at 4°C under vacuum and were rinsed in two changes of buffer. Fixed samples were then dehydrated in a graded ethanol series and embedded in Technovit 7100 resin (Kulzer Histo-technique kit; Labonord) according to Kroes et al. (1998). Specimens were then stored at 37°C. Sections were cut at 3 μm with a Leica RM2165 microtome, mounted on glass slides, stained with toluidine blue, mounted after dehydration in a synthetic resin, and examined with a Leica DM1000 microscope equipped with a Qimaging Micropublisher 3.3 RTV camera.

In the third experiment, the surface of the AZ at 21 DAP was observed using a scanning electron microscope (Phenom G2 Pro; PhenomWorld) and a Coolstage specimen cooling unit (Mk3; PhenomWorld) following fixation in 4% (v/v) glutaraldehyde in phosphate buffer in order to observe the degradation of the middle lamella and the cell walls.

Sugar Determination

Central and L1 pedicels of X3177 were harvested from preselected corymbs at 12, 15, and 20 DAP on the two independent clones. Eight to 10 pedicels were harvested per date and per type (central and L1), and fruit diameter was measured. Pedicels were weighed and individually ground. Sugars were then extracted following the Loudet et al. (2003) protocol. After appropriate dilution, sugar content was assayed by HPLC on a Carbo-pac PA-1 column (Dionex) as described by Rosnoblet et al. (2007).

RNA Purification and Quantification

Total RNA was isolated from five pooled pedicels or AZs using the NucleoSpin RNA Plant extraction kit (Macherey-Nagel) according to the manufacturer's specifications. RNA was then visualized on a 1% (w/v) agarose gel and quantified using the NanoDrop ND-1000 spectrophotometer (NanoDrop Technologies).

Complementary DNA Synthesis and Labeling

A total of 200 ng of RNA was used for the complementary DNA (cDNA) synthesis and amplification using the AMBION MessageAmpII aRNA Amplification kit (Ambion) following the manufacturer's instructions with some modifications as described by Celton et al. (2014a). cDNA and antisense RNA were purified using the AMBION MEGAclear and AMBION DNAclear purification kits, respectively. Antisense RNA was then labeled using Cy3 or Cy5 (Interchim). Purified labeled cDNA was quantified in the NanoDrop ND-1000 spectrophotometer.

Microarray Hybridization, Scanning, and Quantification

The microarray analysis was performed with the NimbleGen ARyANE array containing 126,022 gene-specific probes from apple (Celton et al., 2014a). After 30 pmol of the Cy3 and Cy5 samples was combined and concentrated by precipitation, pellets were resuspended with 2.2 μL of sample-tracking controls and 5.8 μL of hybridization solution. Following a 5-min incubation at 95°C, samples were placed at 42°C prior to loading. Hybridization of the samples to the array was performed overnight on a NimbleGen HS4. Slides were then washed in successive wash buffer and dried before scanning. The arrays were then scanned on a NimbleGen MS 200 scanner.

Experimental Design

Assessment of the Global Transcriptional Profile for Pedicel Vascular Development

Samples harvested at four time points were analyzed in this experiment: E2 stage (2012), F1 stage (2012), 6 DAP (2011), and 12 DAP (2011). For each time point analyzed, two independent biological repeats were performed, with the control and experimental cDNA clones labeled with Cy3 and Cy5 fluorescent dye, respectively. A dye swap was included to eliminate any bias resulting from the two fluorescent dyes. All comparisons were made between the central and L1 flower/fruitlet pedicels at each time point.

Assessment of the Global Transcriptional Profile for AZ Activation and Development

Three AZ developmental stages were analyzed, 14 DAP (2013), 17 DAP (2013), and 21 DAP (2013), using two independent biological repeats. For this experiment, due to the fast-developing AZ observed, a dye-switch analysis was performed to eliminate bias resulting from potential differences between the biological repeats. All comparisons were made between the central and L1 fruitlet AZs at each time point.

Data Normalization and Statistical Analysis

Images were analyzed using DEVA software version 1.2 (Roche). All statistical analyses were performed as described by Celton et al. (2014a) using the R language (R Development Core Team, 2011). Data were first normalized with the lowess method. Normalized intensity values were then subtracted from the background to provide an estimation of the transcript expression levels. Differential expression analyses were performed using the lmFit function and the Bayes-moderated Student's t test using the package LIMMA (Smyth, 2005) from the Bioconductor project. Genes were considered significantly differentially expressed if their P values were $P < 0.05$ for the dye-switch experiment and $P < 0.01$ for the dye-swap experiment. Genes differentially expressed were then screened using a threshold fold change of one or greater. Data clustering was performed using the MapMan software version 3.5.1 (Usadel et al., 2005) using the Euclidian distance and the apple gene annotations. Default statistical parameters were used in those analyses. A cluster number was assigned for K-means clustering analysis to divide data into distinct expression clusters based on the similarity of expression patterns.

The complete microarray data have been deposited at the Gene Expression Omnibus with accession number GSE51729. The subseries GSE51727 regroups information on AZ development, and the subseries GSE51728 regroups information on pedicel vascular development.

RT-qPCR Analyses

Reverse transcription was performed using 1 μg of RNA using the following protocol. RNA sample was denatured for 5 min at 70°C with 1 μL of oligo(dT)$_{15}$ (Promega) and then subjected to reverse transcription with 200 units of Moloney murine leukemia virus-reverse transcriptase (Promega) and 0.5 mM of each deoxyribonucleotide triphosphate in a final volume of 25 μL for 1 h at 42°C. Real-time PCR was performed in triplicate using 3 μL of reverse transcription product in a final volume of 15 μL containing 1× IQ SYBR Green Supermix (Bio-Rad) and 0.2 μM of each primer. Amplifications were performed using an Opticon 4 RealTime PCR detector (Bio-Rad) as follows: 95°C for 3 min, then 40 cycles of 95°C for 15 s and 58°C or 60°C for 1 min. Amplification specificity was checked by a final dissociation curve ranging from 60°C to 95°C. Amplification and dissociation curves were monitored and analyzed with an Opticon Monitor (Bio-Rad). Normalization was performed using three housekeeping genes chosen because of their stability of expression in these samples according to the microarray and subsequent RT-qPCR. The genes chosen for normalization were MDP0000218020, encoding for AGAMOUS-LIKE8, MDP0000927757, encoding for an immunophilin-related protein, and MDP0000217860, putatively encoding for a drought-responsive family protein.

Supplemental Data

The following materials are available in the online version of this article.

Supplemental Figure S1. X3177 fruit drop kinetics according to their position on the corymbs.

Supplemental Figure S2. X3177 fruit volume before shedding.

Supplemental Figure S3. Dynamic X3177 fruit volume for two representative corymbs.

Supplemental Table S1. K-mean clustering of genes differentially expressed between central and lateral 1 fruit pedicels.

Supplemental Table S2. Validation of selected candidate genes differential expression by RT-qPCR.

Supplemental Table S3. K-mean clustering of genes differentially expressed between central and lateral 1 AZs.

ACKNOWLEDGMENTS

We thank the Horticulture Experimental Unit of the Institut National de la Recherche Agronomique (Angers-Nantes), Sylvain Hanteville and Roland Robic for help in the orchard, the I-Mac and Analyse des Acides Nucléiques (Structure Fédérale de Recherche Qualité et Santé du Végétal) platforms for helping with the experiments, Julia Buitink and Soulaiman Sakr for helpful discussions and comments, and Sandra Pelletier and Sylvain Gaillard for help in statistical and microarray analyses.

Received January 17, 2014; accepted February 9, 2014; published February 18, 2014.

LITERATURE CITED

Abot A (2010) Caractérisation des fibres longues de chanvre (*Cannabis sativa*) en vue de leurs utilisations dans des matériaux composites. PhD thesis. Université de Poitier, Poitier, France

Agustí J, Merelo P, Cercós M, Tadeo FR, Talón M (2008) Ethylene-induced differential gene expression during abscission of citrus leaves. J Exp Bot **59:** 2717–2733

Agustí J, Merelo P, Cercós M, Tadeo FR, Talón M (2009) Comparative transcriptional survey between laser-microdissected cells from laminar abscission zone and petiolar cortical tissue during ethylene-promoted abscission in citrus leaves. BMC Plant Biol **9:** 127

Aida M, Ishida T, Tasaka M (1999) Shoot apical meristem and cotyledon formation during Arabidopsis embryogenesis: interaction among the CUP-SHAPED COTYLEDON and SHOOT MERISTEMLESS genes. Development **126:** 1563–1570

Alferez F, Zhong GY, Burns JK (2007) A citrus abscission agent induces anoxia- and senescence-related gene expression in *Arabidopsis*. J Exp Bot **58:** 2451–2462

Aloni R, Feigenbaum P, Kalev N, Rozovsky S (2000) Normonal control of vascular differentiation in plants: the physiological basis of cambium ontogeny and xylem evolution. *In* BJ Savidge, R Napier, eds, Cell and Molecular Biology of Wood Formation. BIOS Scientific Publishers, Oxford, UK, pp 223–236

Avivi Y, Morad V, Ben-Meir H, Zhao J, Kashkush K, Tzfira T, Citovsky V, Grafi G (2004) Reorganization of specific chromosomal domains and activation of silent genes in plant cells acquiring pluripotentiality. Dev Dyn **230:** 12–22

Baima S, Nobili F, Sessa G, Lucchetti S, Ruberti I, Morelli G (1995) The expression of the *Athb-8* homeobox gene is restricted to provascular cells in *Arabidopsis thaliana*. Development **121:** 4171–4182

Baima S, Possenti M, Matteucci A, Wisman E, Altamura MM, Ruberti I, Morelli G (2001) The Arabidopsis ATHB-8 HD-zip protein acts as a differentiation-promoting transcription factor of the vascular meristems. Plant Physiol **126:** 643–655

Bangerth F (2000) Abscission and thinning of young fruit and their regulation by plant hormones and bioregulators. Plant Growth Regul **31:** 43–59

Beisson F, Li-Beisson Y, Pollard M (2012) Solving the puzzles of cutin and suberin polymer biosynthesis. Curr Opin Plant Biol **15:** 329–337

Bonghi C, Tonutti P, Ramina A (2000) Biochemical and molecular aspects of fruitlet abscission. Plant Growth Regul **31:** 35–42

Botton A, Eccher G, Forcato C, Ferrarini A, Begheldo M, Zermiani M, Moscatello S, Battistelli A, Velasco R, Ruperti B, et al (2011) Signaling pathways mediating the induction of apple fruitlet abscission. Plant Physiol **155:** 185–208

Bubán T (2000) The use of benzyladenine in orchard fruit growing: a mini review. Plant Growth Regul **32:** 5961–5966

Cai S, Lashbrook CC (2008) Stamen abscission zone transcriptome profiling reveals new candidates for abscission control: enhanced retention of floral organs in transgenic plants overexpressing Arabidopsis *ZINC FINGER PROTEIN2*. Plant Physiol **146:** 1305–1321

Casson SA, Chilley PM, Topping JF, Evans IM, Souter MA, Lindsey K (2002) The *POLARIS* gene of *Arabidopsis* encodes a predicted peptide required for correct root growth and leaf vascular patterning. Plant Cell **14:** 1705–1721

Celton JM, Gaillard S, Bruneau M, Pelletier S, Aubourg S, Martin-Magniette ML, Navarro L, Laurens F, Renou JP (April 1, 2014a) Widespread anti-sense transcription in apple is correlated with siRNA production and indicates a large potential for transcriptional and/or post-transcriptional control. New Phytol http://dx.doi.org/10.1111/nph.12787

Celton JM, Kelner JJ, Martinez S, Bechti A, Khelifi Touhami A, James MJ, Durel CE, Laurens F, Costes E (2014b) Fruit self-thinning: a trait to consider for genetic improvement of apple. PloS ONE D-13-41379R1 10.1371

Dal Cin V, Barbaro E, Danesin M, Murayama H, Velasco R, Ramina A (2009) Fruitlet abscission: a cDNA-AFLP approach to study genes differentially expressed during shedding of immature fruits reveals the involvement of a putative auxin hydrogen symporter in apple (*Malus domestica* L. Borkh). Gene **442:** 26–36

Dražeta L, Lang A, Cappellini C, Hall AJ, Volz RK, Jameson PE (2004) Vessel differentiation in the pedicel of apple and the effects of auxin transport inhibition. Physiol Plant **120:** 162–170

Duval M, Hsieh TF, Kim SY, Thomas TL (2002) Molecular characterization of AtNAM: a member of the *Arabidopsis* NAC domain superfamily. Plant Mol Biol **50:** 237–248

Eccher G, Botton A, Dimauro M, Boschetti A, Ruperti B, Ramina A (2013) Early induction of apple fruitlet abscission is characterized by an increase of both isoprene emission and abscisic acid content. Plant Physiol **161:** 1952–1969

González-Carranza ZH, Elliott KA, Roberts JA (2007) Expression of polygalacturonases and evidence to support their role during cell separation processes in *Arabidopsis thaliana*. J Exp Bot **58:** 3719–3730

González-Carranza ZH, Whitelaw CA, Swarup R, Roberts JA (2002) Temporal and spatial expression of a polygalacturonase during leaf and flower abscission in oilseed rape and Arabidopsis. Plant Physiol **128:** 534–543

Greene DW, Autio WR, Erf JA, Mao ZY (1992) Mode of action of benzyladenine when used as a chemical thinner on apples. J Am Soc Hortic Sci **117:** 775–779

Hanfrey C, Fife M, Buchanan-Wollaston V (1996) Leaf senescence in Brassica napus: expression of genes encoding pathogenesis-related proteins. Plant Mol Biol **30:** 597–609

Jensen TE, Valdovinos JG (1967) Fine structure of abscission zones. I. Abscission zones of the pedicels of tobacco and tomato flowers at anthesis. Planta **77:** 298–318

Kalaitzis P, Solomos T, Tucker ML (1997) Three different polygalacturonases are expressed in tomato leaf and flower abscission, each with a different temporal expression pattern. Plant Physiol **113:** 1303–1308

Kim J, Jung JH, Reyes JL, Kim YS, Kim SY, Chung KS, Kim JA, Lee MH, Lee Y, Narry Kim V, et al (2005) MicroRNA-directed cleavage of ATHB15 mRNA regulates vascular development in *Arabidopsis* inflorescence stems. Plant J **42:** 84–94

Kim J, Patterson SE (2006) Expression divergence and functional redundancy of polygalacturonases in floral organ abscission. Plant Signal Behav **1:** 281–283

Kiyosue T, Yamaguchi-Shinozaki K, Shinozaki K (1993) Characterization of two cDNAs (ERD11 and ERD13) for dehydration-inducible genes that encode putative glutathione S-transferases in *Arabidopsis thaliana* L. FEBS Lett **335:** 189–192

Kroes GMLW, Baayen RP, Lange W (1998) Histology of root rot of flax seedling (*Linum usitatissimum*) infected by *Fusarium oxyporum* f.sp. *lini*. Eur J Plant Pathol **104:** 725–736

Lakso AN, White MD, Tustin DS (2001) Simulation modeling of the effect of short and long-term climatic variations on carbon balance of apple trees. Acta Hortic **557:** 473–480

Lashbrook CC, Gonzalez-Bosch C, Bennett AB (1994) Two divergent endo-β-1,4-glucanase genes exhibit overlapping expression in ripening fruit and abscising flowers. Plant Cell **6:** 1485–1493

Loescher WH, Marlow GC, Kennedy RA (1982) Sorbitol metabolism and sink-source interconversions in developing apple leaves. Plant Physiol **70:** 335–339

Loudet O, Chaillou S, Krapp A, Daniel-Vedele F (2003) Quantitative trait loci analysis of water and anion contents in interaction with nitrogen availability in *Arabidopsis thaliana*. Genetics **163:** 711–722

Mähönen AP, Bonke M, Kauppinen L, Riikonen M, Benfey PN, Helariutta Y (2000) A novel two-component hybrid molecule regulates vascular morphogenesis of the *Arabidopsis* root. Genes Dev **14:** 2938–2943

Mao L, Begum D, Chuang HW, Budiman MA, Szymkowiak EJ, Irish EE, Wing RA (2000) JOINTLESS is a MADS-box gene controlling tomato flower abscission zone development. Nature **406:** 910–913

Meir S, Philosoph-Hadas S, Sundaresan S, Selvaraj KSV, Burd S, Ophir R, Kochanek B, Reid MS, Jiang CZ, Lers A (2010) Microarray analysis of the abscission-related transcriptome in the tomato flower abscission zone in response to auxin depletion. Plant Physiol **154:** 1929–1956

Nakano T, Fujisawa M, Shima Y, Ito Y (2013) Expression profiling of tomato pre-abscission pedicels provides insights into abscission zone properties including competence to respond to abscission signals. BMC Plant Biol **13:** 40

Ohashi-Ito K, Fukuda H (2003) HD-zip III homeobox genes that include a novel member, ZeHB-13 (Zinnia)/ATHB-15 (*Arabidopsis*), are involved in procambium and xylem cell differentiation. Plant Cell Physiol **44:** 1350–1358

Olsen AN, Ernst HA, Leggio LL, Skriver K (2005) NAC transcription factors: structurally distinct, functionally diverse. Trends Plant Sci **10:** 79–87

Ooka H, Satoh K, Doi K, Nagata T, Otomo Y, Murakami K, Matsubara K, Osato N, Kawai J, Carninci P, et al (2003) Comprehensive analysis of NAC family genes in *Oryza sativa* and *Arabidopsis thaliana*. DNA Res **10:** 239–247

Passarinho PA, Van Hengel AJ, Fransz PF, de Vries SC (2001) Expression pattern of the *Arabidopsis thaliana* AtEP3/AtchitIV endochitinase gene. Planta **212:** 556–567

Patterson SE (2001) Cutting loose: abscission and dehiscence in Arabidopsis. Plant Physiol **126:** 494–500

R Development Core Team (2011) R: A Language and Environment for Statistical Computing. R Foundation for Statistical Computing, Vienna, http://www.R-project.org/ (January 3, 2011)

Ride JP (1978) The role of cell wall alterations in resistance to fungi. Ann Appl Biol **89:** 302–306

Riechmann JL, Heard J, Martin GB, Reuber L, Jiang CZ, Keddie J, Adam L, Pineda O, Ratcliffe OJ, Samaha RR, et al (2000) *Arabidopsis* transcription factors: genome-wide comparative analysis among eukaryotes. Science **290:** 2105–2110

Roberts JA, Elliott KA, González-Carranza ZH (2002) Abscission, dehiscence, and other cell separation processes. Annu Rev Plant Biol **53:** 131–158

Roberts JA, Gonzalez-Carranza ZH (2009) Pectinase function in abscission. Stewart Postharvest Review **5:** 1–4

Roberts JA, Schindler CB, Tucker GA (1984) Ethylene-promoted tomato flower abscission and the possible involvement of an inhibitor. Planta **160:** 159–163

Rolland F, Baena-Gonzalez E, Sheen J (2006) Sugar sensing and signaling in plants: conserved and novel mechanisms. Annu Rev Plant Biol **57:** 675–709

Rosnoblet C, Aubry C, Leprince O, Vu BL, Rogniaux H, Buitink J (2007) The regulatory gamma subunit SNF4b of the sucrose non-fermenting-related kinase complex is involved in longevity and stachyose accumulation during maturation of *Medicago truncatula* seeds. Plant J **51:** 47–59

Ruperti B, Bonghi C, Ziliotto F, Pagni S, Rasori A, Varotto S, Tonutti P, Giovannoni JJ, Ramina A (2002) Characterization of a major latex protein (MLP) gene down-regulated by ethylene during peach fruitlet abscission. Plant Sci **163:** 265–272

Ruperti B, Whitelaw CA, Roberts JA (1999) Isolation and expression of an allergen-like mRNA from ethylene-treated *Sambucus nigra* leaflet abscission zones. J Exp Bot **50:** 733–734

Sachs T (1981) The control of the patterned differentiation of vascular tissues. Adv Bot Res **9:** 151–262

Scheible WR, Morcuende R, Czechowski T, Fritz C, Osuna D, Palacios-Rojas N, Schindelasch D, Thimm O, Udvardi MK, Stitt M (2004) Genome-wide reprogramming of primary and secondary metabolism, protein synthesis, cellular growth processes, and the regulatory infrastructure of Arabidopsis in response to nitrogen. Plant Physiol **136:** 2483–2499

Schuetz M, Smith R, Ellis B (2013) Xylem tissue specification, patterning, and differentiation mechanisms. J Exp Bot **64:** 11–31

Seo HS, Song JT, Cheong JJ, Lee YH, Lee YW, Hwang I, Lee JS, Choi YD (2001) Jasmonic acid carboxyl methyltransferase: a key enzyme for jasmonate-regulated plant responses. Proc Natl Acad Sci USA **98:** 4788–4793

Smyth GK (2005) LIMMA: linear models for microarray data. *In* R Gentleman, S Dudoit, R Irizarry, W Huber, eds, Bioinformatics and Computational Biology Solutions using R and Bioconductor. Springer, New York, pp 397–420

Steeves TA, Sussex IM (1989) Patterns in Plant Development. Cambridge University Press, Cambridge, UK

Szekeres M, Németh K, Koncz-Kálmán Z, Mathur J, Kauschmann A, Altmann T, Rédei GP, Nagy F, Schell J, Koncz C (1996) Brassinosteroids rescue the deficiency of CYP90, a cytochrome P450, controlling cell elongation and de-etiolation in *Arabidopsis*. Cell **85:** 171–182

Takei K, Ueda N, Aoki K, Kuromori T, Hirayama T, Shinozaki K, Yamaya T, Sakakibara H (2004) AtIPT3 is a key determinant of nitrate-dependent cytokinin biosynthesis in *Arabidopsis*. Plant Cell Physiol **45:** 1053–1062

Taylor JE, Whitelaw CA (2001) Signal in abscission. New Phytol **151:** 323–339

Usadel B, Nagel A, Thimm O, Redestig H, Blaesing OE, Palacios-Rojas N, Selbig J, Hannemann J, Piques MC, Steinhauser D, et al (2005) Extension of the visualization tool MapMan to allow statistical analysis of arrays, display of corresponding genes, and comparison with known responses. Plant Physiol **138:** 1195–1204

van Doorn WG, Stead AD (1997) Abscission of flowers and floral parts. J Exp Bot **48:** 821–837

Wang RC, Okamoto M, Xing XJ, Crawford NM (2003) Microarray analysis of the nitrate response in Arabidopsis roots and shoots reveals over 1,000 rapidly responding genes and new linkages to glucose, trehalose-6-phosphate, iron, and sulfate metabolism. Plant Physiol **132:** 556–567

Webster BD (1968) Anatomical aspects of abscission. Plant Physiol **43:** 1512–1544

Wilson WC, Hendershott CH (1968) Anatomical and histochemical studies of abscission of oranges. J Am Soc Hortic Sci **92:** 203–210

Wingler A, Masclaux-Daubresse C, Fischer AM (2009) Sugars, senescence, and ageing in plants and heterotrophic organisms. J Exp Bot **60:** 1063–1066

Wingler A, Roitsch T (2008) Metabolic regulation of leaf senescence: interactions of sugar signalling with biotic and abiotic stress responses. Plant Biol (Stuttg) (Suppl) **10:** 50–62

Yamamoto R, Demura T, Fukuda H (1997) Brassinosteroids induce entry into the final stage of tracheary element differentiation in cultured Zinnia cells. Plant Cell Physiol **38:** 980–983

Zhang J, Liu H, Sun J, Li B, Zhu Q, Chen S, Zhang H (2012) *Arabidopsis* fatty acid desaturase FAD2 is required for salt tolerance during seed germination and early seedling growth. PLoS ONE **7:** e30355

Zhao C, Craig JC, Petzold HE, Dickerman AW, Beers EP (2005) The xylem and phloem transcriptomes from secondary tissues of the Arabidopsis root-hypocotyl. Plant Physiol **138:** 803–818

Zhong R, McCarthy RL, Lee C, Ye ZH (2011) Dissection of the transcriptional program regulating secondary wall biosynthesis during wood formation in poplar. Plant Physiol **157:** 1452–1468

Zhong R, Taylor JJ, Ye ZH (1999) Transformation of the collateral vascular bundles into amphivasal vascular bundles in an Arabidopsis mutant. Plant Physiol **120:** 53–64

Zhou C, Lakso AN, Robinson TL, Gan S (2008) Isolation and characterization of genes associated with shade-induced apple abscission. Mol Genet Genomics **280:** 83–92

Zhou GK, Kubo M, Zhong R, Demura T, Ye ZH (2007) Overexpression of miR165 affects apical meristem formation, organ polarity establishment and vascular development in Arabidopsis. Plant Cell Physiol **48:** 391–404

Zhu H, Dardick CD, Beers EP, Callanhan AM, Xia R, Yuan R (2011) Transcriptomics of shading-induced and NAA-induced abscission in apple (Malus domestica) reveals a shared pathway involving reduced photosynthesis, alterations in carbohydrate transport and signaling and hormone crosstalk. BMC Plant Biol **11:** 138